Age and synchronicity of planktonic foraminiferal bioevents across the Cenomanian–Turonian boundary interval (middle Cretaceous)

Francesca Falzoni[a]*, Maria Rose Petrizzo[a], Michèle Caron[b], R. Mark Leckie[c], Khalifa Elderbak[c,d]

[a]Dipartimento di Scienze della Terra "A. Desio", Università degli Studi di Milano, via Mangiagalli 34, 20133 Milano, Italy.

[b]Département de Geosciences, Institut de Géologie, Université de Fribourg, Pérolles, 1700 Fribourg, Switzerland.

[c]Department of Geosciences, University of Massachusetts-Amherst, Amherst, Massachusetts 01003, USA.

[d]ALS, Houston, Texas, USA.

*Corresponding author. E-mail: francesca.falzoni@unimi.it, phone: +39-0250315563; Fax: +39-0250315494

Abstract

The upper Cenomanian–lower Turonian is a key-stratigraphic interval, as it encompasses the mid-Cretaceous supergreenhouse and a major perturbation of the global carbon cycle (i.e., Oceanic Anoxic Event 2) as evidenced by a global positive carbon isotope excursion and by the nearly world-wide deposition of organic-rich marine facies. A turnover in planktonic foraminiferal

assemblages and in other marine organisms is documented across this stratigraphic interval, but reconstruction of the timing and identification of the cause and effect relationships between environmental perturbations and organism response require a highly-resolved stratigraphic framework. The appearance and extinction levels of planktonic foraminiferal species generally allow accurate intra- and supra-basinal correlations. However, bioevents cannot be assumed to be globally synchronous, because the stratigraphic and geographic distribution of species is modulated by the ecological preferences exhibited by each taxon and controlled by the oceanic circulation, often resulting in earlier or delayed events in certain geographic areas.

The aim of this study is to test the synchronicity of the planktonic foraminiferal bioevents recognized across the C/T boundary and to provide the most reliable sequence of events for correlation of mid- to low latitude localities. For this purpose, we have completed a highly-resolved biostratigraphic analysis of the European reference section for the C/T boundary at Eastbourne, Gun Gardens (UK), and of core S57, (Tarfaya, Morocco) and correlated the sequence of bioevents identified with those recorded in other coeval sections available in the literature, including the GSSP section for the base of the Turonian Stage at Rock Canyon, Pueblo (Colorado), where we calculate reliable estimates of planktonic foraminiferal events that are well-constrained by radioisotopically and astrochronologically dated bentonite layers.

Results indicate that the extinctions of *Thalmanninella deeckei*, *Thalmanninella greenhornensis*, *Rotalipora cushmani* and "*Globigerinelloides*" *bentonensis* in the latest Cenomanian are reliable bioevents for correlation. In addition, our analysis highlights other promising lowest occurrences (LOs) that, however, need to be better constrained by bio- and chemostratigraphy, including the LO *Marginotruncana schneegansi* falling close to the C/T boundary. By contrast, the appearance of *Helvetoglobotruncana helvetica* and of some *Dicarinella*

47 species, the onset of the "*Heterohelix*" shift and the extinction of anaticinellids are clearly
48 diachronous across mid-low latitude localities. Finally, our study suggests that different species
49 concepts among authors, different sample size and sampling resolution, as well as species
50 paleoecology are important factors that control the stratigraphic position at which bioevents are
51 identified.
52
53 **Keywords: Cenomanian–Turonian, stratigraphy, mid-low latitude correlations, planktonic**
54 **foraminifera, Pueblo, Eastbourne.**
55
56 **1. Introduction**
57
58 The Cenomanian–Turonian boundary interval (middle Cretaceous) represents one of the most
59 interesting case-studies for investigating the evolution of the marine biota under the intense
60 environmental perturbations that occurred during Oceanic Anoxic Event 2 (e.g., Schlanger and
61 Jenkyns, 1976; Scholle and Arthur, 1980; Schlanger et al., 1987). In fact, OAE 2 is globally
62 recognized as a time of increased sea-surface productivity under greenhouse climate conditions
63 interrupted by a brief cooling episode (i.e., the "Plenus Cold Event", see Gale and Christensen,
64 1996; Forster et al., 2007; Sinninghe Damsté et al., 2010; Jarvis et al., 2011; Jenkyns et al., 2017
65 among others) that may correspond to a re-oxygenation event of bottom waters in the Western
66 Interior Seaway (WIS) (i.e., the "benthonic zone": Eicher and Worstell, 1970; Elderbak and Leckie,
67 2016). Across OAE 2, planktonic foraminiferal assemblages underwent a substantial re-
68 organization that led to the extinction of the single-keeled rotaliporids with umbilical supplementary
69 apertures (genera *Rotalipora* and *Thalmanninella*) and to the appearance and progressive

diversification of double-keeled taxa (genera *Dicarinella* and *Marginotruncana*), that dominated the assemblages until the Santonian (e.g., Robaszynski et al., 1990, 1993; Premoli Silva and Sliter, 1999; Leckie et al., 2002; Falzoni et al., 2013, 2016a; Petrizzo et al., 2017). However, correlating stratigraphic sequences, extrapolating global from local signals, and reconstructing the cause and effect relationships between environmental changes and organism response require a reproducible and highly-resolved stratigraphic framework. Unfortunately, the C–T boundary interval lacks magnetostratigraphic control, being within the Cretaceous Normal Superchron (e.g., Gradstein et al., 2012). Nevertheless, this interval is accompanied by a ~+2‰ excursion in both the $\delta^{13}C_{carb}$ and $\delta^{13}C_{org}$ resulting from the burial of organic matter during OAE 2 (e.g., Jenkyns, 2010). The shape of the $\delta^{13}C$ profile with its typical peaks and troughs represents one of the most reproducible features of this stratigraphic interval, and being likely synchronously registered in the marine and continental records, it represents a powerful tool for global correlation (e.g., Pratt and Threlkeld, 1984; Tsikos et al., 2004; Jarvis et al., 2006, 2011; Jenkyns, 2010).

Planktonic foraminiferal bioevents are routinely applied to correlate pelagic and hemipelagic successions, and their contribution to implement the accuracy and resolution of the Geologic Time Scale is particularly important since the Early Cretaceous. However, despite this group of pelagic organisms having a wide distribution, each living/fossil species possesses ecologic preferences that may control its geographic and stratigraphic distribution. Consequently, planktonic foraminiferal bioevents cannot be assumed to be globally synchronous and their reliability for correlation requires testing through other relative dating techniques. For instance, the identification of the Cenomanian/Turonian boundary based on planktonic foraminiferal events is problematic. In fact, the base of the Turonian Stage is formally defined by the lowest occurrence (LO) of the ammonite *Watinoceras devonense* at the GSSP section at Rock Canyon, Pueblo, Colorado (Kennedy et al.,

93 2000, 2005). However, ammonites are often rare or absent in hemipelagic and pelagic successions,
94 thus the identification of the C/T boundary in the absence of the primary marker is based on
95 secondary bioevents, including the LO of *Helvetoglobotruncana helvetica* among planktonic
96 foraminifera. However, the appearance of *H. helvetica* is known to be an unreliable event to
97 approximate the base of the Turonian, because of its diachronous occurrence, rarity in the lower
98 part of its stratigraphic distribution, very transitional evolution from its ancestor
99 *Helvetoglobotruncana praehelvetica*, and absence or very rare occurrence in epicontinental margin
100 settings (e.g., Hart and Carter, 1975; Carter and Hart, 1977; Hart and Weaver, 1977; Hart and Bigg,
101 1981; Leckie, 1985; Hilbrecht et al., 1986; Jarvis et al., 1988; Lipson-Benitah et al., 1988;
102 Robaszynski et al., 1990; Kuhnt et al., 1997; Keller et al., 2001; Luciani and Cobianchi, 1999; Tur
103 et al., 2001; Petrizzo, 2001; Holbourn and Kuhnt, 2002; Caron et al., 2006; Mort et al., 2007;
104 Desmares et al., 2007; Hart, 2008; Gebhardt et al., 2010; Huber and Petrizzo, 2014). Further
105 complication is introduced by inconsistencies in the stratigraphic position of planktonic
106 foraminiferal events, including the identification of LOs and HOs of marker taxa (e.g., *Rotalipora*
107 *cushmani*, *H. helvetica*), when the same section is studied by different authors (Pueblo: Eicher and
108 Diner, 1985; Leckie, 1985; Leckie et al., 1998; Keller and Pardo, 2004; Caron et al., 2006;
109 Desmares et al., 2007; Elderbak and Leckie, 2016; Eastbourne: Paul et al., 1999; Keller et al., 2001;
110 Hart et al., 2002; Tsikos et al., 2004).
111 The aim of this study is to select the most reliable and replicable sequence of planktonic
112 foraminiferal bioevents across the C–T boundary interval, by distinguishing between the most
113 trustworthy isochronous bioevents from those that instead are more regional or diachronous in
114 nature. The section of Eastbourne at Gun Gardens and core S57 (Tarfaya Basin) were here re-
115 studied at high-resolution to complement the planktonic foraminiferal data published in Tsikos et al.

(2004). Firstly, we developed a well-constrained age-model of the Pueblo (Rock Canyon) to obtain numerical estimates of planktonic foraminiferal events recognized in the GSSP section. Subsequently, we tested the synchronicity of each bioevent by performing graphic correlations between Pueblo (Rock Canyon) and Eastbourne (Gun Gardens) and between Pueblo (Rock Canyon) and Tarfaya (Core S57), and by comparing the stratigraphic position of each bioevent respect to the peaks and troughs of the $\delta^{13}C$ profile in other mid-low latitude localities available in the literature, selected among those yielding the most complete stratigraphic record and a highly resolved $\delta^{13}C$ profile. Italian sections are only briefly discussed, because of the absence of planktonic foraminifera in the black shale layers (e.g., Premoli Silva and Sliter, 1995; Premoli Silva et al., 1999; Coccioni and Luciani, 2004, 2005; Coccioni and Premoli Silva, 2015), and of the stratigraphic gap across the Bonarelli Level and time equivalent organic-rich facies (Gambacorta et al., 2015).

2. Materials and Methods

To document the sequence of planktonic foraminiferal bioevents across the C–T boundary interval, we have examined samples from (1) Eastbourne, Gun Gardens, UK, and (2) core S57 drilled in the Tarfaya Basin (Morocco), and paleogeographically located in the Anglo-Paris Basin and central Atlantic Ocean, respectively (Tsikos et al., 2004; Fig. 1). The Eastbourne section yields the most expanded C–T boundary interval of the English Chalk and represents the European reference section for the C/T boundary (Paul et al., 1999). Planktonic foraminifera have been object of a number of studies (Paul et al., 1999; Keller et al., 2001; Hart et al., 2002; Tsikos et al., 2004) and the section at Gun Gardens has been restudied to verify the discrepancies observed in the identification of species and position of the bioevents (including zonal markers). The sampling resolution adopted here for the biostratigraphic analysis is 20 cm throughout the section at

139 Eastbourne, and between 20 and 50 cm at Tarfaya. Rock samples from core S57 (Tarfaya) and from
140 the Plenus Marls Member (Eastbourne) have been processed with peroxide water to obtain washed
141 residues. Novelty of this study compared to Tsikos et al. (2004) is introduced by the disaggregation
142 of chalk samples from the Grey Chalk, Ballard Cliff and Holywell Members (Eastbourne) with
143 acetic acid (80%) and water (20%) to obtain washed residues yielding well-preserved isolated
144 specimens (see Lirer, 2000 and Falzoni et al., 2016b for detailed procedure), a procedure also used
145 by Elderbak and Leckie (2016) for the hard limestones at the Rock Canyon section.
146 In order to compare our biostratigraphic results with those from other localities, we have
147 selected the most complete stratigraphic sequences spanning the C–T boundary interval and having
148 detailed planktonic foraminiferal biostratigraphic data, as well as a highly-resolved $\delta^{13}C_{carb}$ or
149 $\delta^{13}C_{org}$ profile: WIS: (1) Rock Canyon, Pueblo, Colorado (Eicher and Diner, 1985; Leckie, 1985;
150 Leckie et al., 1998; Keller and Pardo, 2004; Caron et al., 2006; Desmares et al., 2007; Elderbak and
151 Leckie, 2016); Vocontian Basin: (2) Clot Chevalier (Falzoni et al., 2016b) and (3) Pont d'Issole
152 (Grosheny et al., 2006), SE France; Tethyan Ocean: (4) wadi Bahloul, Tunisia (Caron et al., 2006);
153 Indian Ocean: (5) Gongzha, Tibet (Bomou et al., 2013) (Fig. 1). In addition, planktonic
154 foraminiferal bioevents identified in these localities are briefly discussed by comparing their
155 stratigraphic position with other classic C/T boundary sections, where the $\delta^{13}C$ profile is not
156 available. The published litho-, bio-, and chemostratigraphic data of Clot Chevalier, Pont d'Issole,
157 wadi Bahloul, and Gongzha are reproduced in the Supplementary Materials (Supplementary Figs.
158 A-D). Source of data for each section and the methodology applied to study the planktonic
159 foraminifera (thin sections, washed residues or a combination of both) are listed in Table 1.
160 Taxonomic concepts for planktonic foraminiferal species identification follow their original
161 descriptions and illustrations, the online taxonomic database for Mesozoic planktonic foraminifera

162 **"**PF@Mikrotax**"** available at http://www.mikrotax.org/pforams/index.html, Robaszynski et al.
163 (1979) and Falzoni et al. (2016b). Genera attribution is according to the taxonomic revision by
164 Gonzalez Donoso et al. (2007) for rotaliporids and Haynes et al. (2015) for biserial taxa. Species
165 mentioned in the text and/or in the figures are listed in the Taxonomic Appendix. The planktonic
166 foraminiferal biozonation is according to Sliter (1989) and Robaszynski and Caron (1995).
167
168 **3. Remarks on the planktonic foraminiferal record at Pueblo (Colorado)**
169 The GSSP for the base of the Turonian Stage is located at the Rock Canyon section at Pueblo
170 (Colorado). The primary marker for the identification of the base of the Turonian is the LO of the
171 ammonite *Watinoceras devonense* in bed 86 (Kennedy et al., 2000, 2005) (Fig. 2). According to the
172 GSSP definition, additional secondary bioevents include the LO of the calcareous nannofossil
173 *Quadrum gartneri*, which almost coincides with the C/T boundary as defined by ammonite
174 stratigraphy at Pueblo (Tsikos et al., 2004), and the LO of the planktonic foraminifera
175 *Helvetoglobotruncana helvetica*.
176 Planktonic foraminifera at Pueblo have been studied numerous times over the last 45 years
177 with different sampling resolution (Eicher and Worstell 1970; Eicher and Diner, 1985, Leckie,
178 1985, Leckie et al., 1998; Keller and Pardo, 2004; Keller et al., 2004; Caron et al. 2006; Desmares
179 et al., 2007; Elderbak and Leckie, 2016). Almost all the above-mentioned studies [with the
180 exception of Eicher and Worstell (1970), where the planktonic foraminiferal biozonation is not
181 discussed] assigned the sedimentary succession outcropping at Rock Canyon to the three planktonic
182 foraminiferal biozones according to the subtropical biozonation by Sliter (1989) and Robaszynski
183 and Caron (1995): *R. cushmani*, *Whiteinella archaeocretacea* and *H. helvetica* Zones. However,
184 some discrepancies can be found in the identification of the zonal markers, as follows: the HO of *R.*

185 *cushmani* is identified in Bed 65 (Kennedy et al., 2005 after Eicher and Diner, 1985), in Bed 66
186 (Keller and Pardo, 2004), and within Bed 68 (Leckie, 1985; Caron et al., 2006). Desmares et al.
187 (2007) identified atypical morphotypes of *R. cushmani* (i.e., with a "discrete peripheral keel, which
188 is sometimes not expressed on each chamber or is even totally absent") up to Bed 85. Leckie (1985)
189 also reported a single occurrence of *R. cushmani* as high as the upper part of Bed 85, but with a
190 significant stratigraphic gap between this and the presumed HO of *R. cushmani* in Bed 68 (below
191 Bentonite A). The 3.5-m gap between relatively rare but consistent presence of *R. cushmani* up to
192 Bed 68, followed by no specimens, and then extremely sparse presence in the upper part of Bed 85
193 begs a question about reworking.
194 There are also major inconsistencies with regard to the position of the LO of *H. helvetica*,
195 which is identified in Bed 86 by Desmares et al. (2007), in Bed 89 by Keller and Pardo (2004) and
196 Kennedy et al. (2005) after Eicher and Diner (1985), in Bed 102 by Caron et al. (2006), and in
197 limestone Bed 103 by Elderbak and Leckie (2016). It should be noted here that three-dimensional
198 specimens of foraminifera were extracted and analyzed from calcareous shales, marlstones, and
199 limestones in the study by Elderbak and Leckie (2016). Based on the above, we placed the top of
200 the *R. cushmani* Zone according to Leckie (1985), representing the youngest record of the species,
201 with the exception of the possibly reworked specimens within Bed 85, and the base of the *H.*
202 *helvetica* Zone according to Elderbak and Leckie (2016) (Fig. 2).
203
204 **4. Re-interpretation of A, B, and C peaks on the $\delta^{13}C$ profile**
205 Several $\delta^{13}C_{carb}$ and $\delta^{13}C_{org}$ records have been generated for the Rock Canyon section and for cores
206 drilled nearby over the last 30 years (Pratt and Threlkeld, 1984; Pratt, 1985; Pratt et al., 1993;
207 Keller et al., 2004; Bowman and Bralower, 2005; Caron et al., 2006; Sageman et al., 2006). In Fig.

208 2, we have plotted the $\delta^{13}C_{carb}$ obtained from outcrop samples at the GSSP section (Caron et al.,
209 2006) and the $\delta^{13}C_{org}$ profiles obtained from the PU-79 core (Pratt and Threlkeld, 1984; Pratt, 1985).
210 The $\delta^{13}C_{org}$ curve by Pratt and Threlkeld (1984) and Pratt (1985) was later reproduced by other
211 authors including Kennedy et al. (2005) in the paper where the GSSP for the base of the Turonian
212 Stage was defined, with some discrepancies compared to the original version (see Caron et al., 2006
213 for discussion).
214 Pratt and Threlkeld (1984) and Pratt (1985) described peaks A, B, C as follows: "A= initial rapid
215 increase in values and first peak; B= notch caused by brief decrease in values; C= second increase
216 and plateau of values", meaning that Pratt and Threlkeld (1984) originally interpreted peak A as a
217 maximum, peak B as a trough and peak C as the entire plateau of positive (= less negative) values
218 above B rather than a single point of the $\delta^{13}C$ profile (Fig. 2). However, different criteria have been
219 successively adopted for the identification of the peaks first identified by Pratt and Threlkeld
220 (1984). For instance, the position of the carbon isotope peaks in the Demerara Rise record
221 (Erbacher et al., 2005; Leg 201, Central Atlantic Ocean) has been interpreted as follows: peaks A
222 and B are troughs, C is the positive peak, and a fourth maximum point (named D) is recognized
223 below the decrease of the $\delta^{13}C$ to pre-excursion values. By contrast, Jarvis et al. (2006, 2011)
224 named A, B and C the three $\delta^{13}C_{carb}$ maxima across the C–T boundary interval in a composite
225 isotope curve of the English chalk, with peak C falling very close to the C/T boundary. Voigt et al.
226 (2007, 2008) adopted the same criteria but also recognized a fourth positive peak above the C/T
227 boundary that they named D. These latter schemes were followed by a number of authors in recent
228 years (e.g., Pearce et al., 2009; Westermann et al., 2010; Bomou et al., 2013; Eldrett et al., 2015;
229 Falzoni et al., 2016b) resulting in the common practice of approximating the C/T boundary to point
230 C (as interpreted by Jarvis et al., 2006) in the absence of *W. devonense*. Other authors preferred to

number the observed maxima of the $\delta^{13}C$ profile as I, II, and III (e.g., Caron et al., 2006; Grosheny et al., 2006).

Based on the observations above, the position of the carbon isotope peaks A, B, and C is here summarized in order to univocally compare and correlate the planktonic foraminiferal bioevents across the stratigraphic sections discussed in this study. Therefore, considering previous interpretations and according to Jarvis et al. (2006, 2011), we identify three positive points (A, B, C) and a plateau of high $\delta^{13}C_{carb}$ and $\delta^{13}C_{org}$ values, having a small offset, between B and C, and specifically, A is the initial rapid increase in values and first peak (as originally defined by Pratt and Threlkeld, 1984, and Pratt, 1985), B is the second positive peak of $\delta^{13}C$, following a decrease in values, and beginning of the plateau and is usually represented by multiple $\delta^{13}C$ points, and C is the last positive peak of the plateau before the carbon-isotope profile gradually decreases to pre-excursion values. Nevertheless, uncertainties might remain on the identification of A, B, C peaks in some localities, because of the presence of additional peaks and troughs due to local variations of the $\delta^{13}C$ content and/or to diagenesis that might complicate the apparently simple structure of the $\delta^{13}C$ profile and/or to a different sampling resolution. For instance, point C (i.e., the last positive peak of the plateau before the $\delta^{13}C$ decreases to pre-excursion values) at Eastbourne might be placed in two different positions, i.e., (1) at the transition between the Ballard Cliff and the Holywell Member according to Jarvis et al. (2006), or (2) near the top of the Ballard Cliff Member according to Voigt et al. (2008) (Fig. 3). Moreover, slight discrepancies in the stratigraphic position of peaks and troughs on the $\delta^{13}C_{carb}$ and $\delta^{13}C_{org}$ profiles are often observed in case both curves are available for the same section (e.g., Pueblo, Eastbourne).

5. Results

254

255 *5.1. Eastbourne, Gun Gardens (UK)*

256 Planktonic foraminiferal events identified at Eastbourne (Gun Gardens) in this study and those
257 available in the literature (Paul et al., 1999; Keller et al., 2001; Hart et al., 2002; Tsikos et al., 2004)
258 are combined with the available carbon isotope records (Paul et al., 1999; Tsikos et al., 2004) and
259 plotted against stratigraphy (Fig. 3).

260 The HO of *R. cushmani* (Fig. 4, 1a–c) is recorded at top of Bed 3 (Keller et al., 2001) or
261 within Bed 4 of the Plenus Marls Member (Paul et al., 1999; Hart et al., 2002; Tsikos et al., 2004),
262 in agreement with this study, while the LO of *H. helvetica* is identified at the top of the Ballard Cliff
263 (Keller et al., 2001) or at the base of the Holywell Member (Hart et al., 2002) (Fig. 3). By contrast,
264 we do not record the occurrence of the latter species throughout the section, in agreement with Paul
265 et al. (1999) and Tsikos et al. (2004). Consequently, the succession studied is assigned to the *R.*
266 *cushmani* (from 0 to 11.4 m) and to the overlying *W. archaeocretacea* Zone (from 11.4 to 26 m)
267 (Fig. 3), according to Tsikos et al. (2004).

268 Based on our biostratigraphic analysis, *Praeglobotruncana algeriana* (Fig. 4, 2a–c),
269 *Dicarinella hagni* (Fig. 4, 3a–c), and *Dicarinella imbricata* (Fig. 4, 4a–c) occur from the base of the
270 section, therefore their LOs likely fall in older stratigraphic intervals. Additional planktonic
271 foraminiferal events identified in the Grey Chalk are listed below in stratigraphic order: 1) the LO
272 of *H. praehelvetica* (Fig. 4, 5a–c) at 2.4 m above the base of the section; 2) the LO of *Dicarinella*
273 *canaliculata* at 3.2 m; and 3) the LO of *Dicarinella elata* (Fig. 4, 6a–c) at 4.0 m. The following
274 events are identified in the Plenus Marls Member: 1) the HO of *Thalmanninella brotzeni* (Fig. 4,
275 7a–c) at 7.2 m above the base of the section; 2) the HO of *Thalmanninella greenhornensis* (Fig. 4,
276 8a–c) and of 3) *Thalmanninella deeckei* (Fig. 4, 9a–c) at 8.2 m within Bed 1; 4) the LO of

277 *Praeglobotruncana oraviensis* (Fig. 4, 10a–c) at 8.8 m, and 5) the HO of *Rotalipora montsalvensis*
278 (Fig. 5, 1a–c) at 9.2 m within Bed 2; 6) the HO of *Rotalipora praemontsalvensis* (Fig. 5, 2a–c) at 10
279 m within Bed 3; and 7) the HO of "*Globigerinelloides" bentonensis* at 13 m within Bed 7 (Fig. 3).
280 Specimens that fall in the range of variability of *W. archaeocretacea* (Fig. 5, 3a–c) are identified
281 from 0.6 m above the base of the section, but occur rarely in the assemblage and show an extremely
282 scattered stratigraphic distribution, therefore their first appearance at 0.6 m may not correspond to
283 its LO in the English Chalk. No noteworthy planktonic foraminiferal bioevents have been identified
284 in the White Chalk Formation. The C/T boundary is here placed at the base of the *W. devonense*
285 Zone according to Gale et al. (2005), however, it is worth mentioning that the ammonite species *W.*
286 *devonense* is not identified at Eastbourne and the *W. devonense* Zone is recognized based on the
287 occurrence of other coeval ammonite species (Paul et al., 1999; Gale et al., 2005).
288
289 *5.2 Tarfaya* (*core S57)*
290 The sedimentary succession studied is assigned to the *R. cushmani* (from the base of the core to
291 50.96 m) and to the overlying *W. archaeocretacea* Zone (from 50.96 m to the top of the cored
292 interval), according to Tsikos et al. (2004). The occurrence of *H. helvetica* is not recorded
293 throughout the stratigraphic interval examined (Fig. 6). Planktonic foraminiferal bioevents
294 identified in this study are listed in stratigraphic order: (1) LO of *H. praehelvetica* (54.91 m) (Fig. 5,
295 4a–c), (2) HO of *Th. deeckei* (54.16 m) (Fig. 5, 5a–c), (3) HO of *Th. greenhornensis* (53.96 m) (Fig.
296 5, 6a–c), and (4) HO of *"G". bentonensis* (50.16 m) (Fig. 5, 7a–c). The "*Heterohelix* shift"
297 (abundance of biserial taxa > 50% *sensu* Leckie et al., 1998) is recorded from 50.16 m. Biserial
298 taxa, mainly *Planoheterohelix moremani* (Fig. 5, 8a–b) and *Planoheterohelix paraglobulosa* (Fig. 5,
299 9a–b) dominate the assemblage up to the top of the core. *Praeglobotruncana algeriana* (Fig. 5,

10a–c), *Dicarinella hagni* (Fig. 5, 11a–c), and *Dicarinella imbricata* occur from the bottom of the core. The C/T boundary is here approximate to fall between peak C on the $\delta^{13}C_{org}$ profile and the LO of *Q. gartneri* according to Tsikos et al. (2004).

6. Discussion

6.1 Age-depth model for the Pueblo section

Bentonites occurring in the Portland Core (Pueblo) were accurately and precisely dated by intercalibrating radioisotopic and astrochronologic time scales (Meyers et al., 2012). This study also concluded that bentonites found in the same ammonite biozone in different localities of the WIS across the C–T boundary interval have a common eruptive origin and are isochronous. Therefore, we used the age of bentonites obtained by Meyers et al. (2012) to calculate a reliable estimate of planktonic foraminiferal species first and last appearances data in the Rock Canyon section (Fig. 7). The age of the bentonites used to develop the age-model and the age of the bioevents extrapolated in this study are listed in Table 2. The calculated ages for the LO of *P. algeriana*, *D. hagni*, *D. elata*, *D. canaliculata*, *D. imbricata,* for the HO of *Th. deeckei*, and for the LO of *H. praehelvetica* (base of the section) and for the LO of *M. marianosi* and *H. helvetica* (top of the section) include a higher margin of error, because these events fall outside the interval constrained by bentonites, although they are aligned to the line of correlation. The age of *M. sigali* was not calculated, because it falls in an interval where the sedimentation rate might have been significantly different (see Fig. 2). The HO of *Th. multiloculata* and of *R. planoconvexa* and of the atypical *R. cushmani* could not

322 be calculated because of the unavailability of the precise sample depth at which these events are
323 recognized.
324 The age obtained for the HO of *R. cushmani* (94.29 Ma) is 10 kyr younger than those derived from
325 the work by Robaszynski et al. (1998) in the Anglo-Paris Basin and reported in the GTS 2012
326 (Gradstein et al., 2012). Because the age estimate in the GTS 2012 was not well calibrated due to
327 the uncertain HO of *R. cushmani* at Gubbio and in the Moroccan record (see Anthonissen and Ogg,
328 2012), our calculated age for this event represents a more reliable estimate of its extinction, as it is
329 falls very close to bentonite A. This age estimate represents a good approximation for the HO of *R.*
330 *cushmani* across mid-low latitudes, with the exception of the Moroccan record where the
331 interpretation of its apparently delayed extinction requires further studies (see discussion in
332 paragraphs 6.1.2 and 6.3.1). The LO of *H. helvetica* at 93.48 Ma is also slightly younger (40 kyr)
333 than previously estimated (GTS 2012; Gradstein et al., 2012), but because of the clearly
334 diachronous nature of this event, this age cannot be applied to other localities. The LO of *D.*
335 *imbricata* clearly precedes the extinction of *R. cushmani* at Rock Canyon and in other localities (see
336 discussion below) and the age derived for its appearance in the GSSP section (94.51 Ma) is
337 significantly older (310 kys) than estimated in the GTS 2012 (Gradstein et al., 2012), where this
338 events is reported to occur above the HO of *R. cushmani*. Finally, it is worth noting that the
339 extinction of *Th. greenhornensis* is significantly delayed at Pueblo compared to other mid-low
340 latitude records (see paragraph 6.4.1 and Fig. 9), therefore the age obtained in this study has to be
341 recalibrated in other localities.
342
343 *6.2. Graphic correlations*

344 To test the synchronism of events and the accuracy of correlations among sections, we performed
345 graphic correlations of Pueblo *vs*. Eastbourne (Fig. 8a) and Pueblo *vs*. Tarfaya (Fig. 8b) (e.g., Shaw,
346 1964; Sadler, 2004; Paul and Lamolda, 2009; Petrizzo et al., 2011). To increase the number of
347 common events, we integrate planktonic foraminiferal datums with the calcareous nannofossil,
348 ammonite, and chemostratigraphic events (peaks A, B and C of the $\delta^{13}C$ profile) available in the
349 literature. Moreover, we considered the two interpretations regarding the position of peak C at
350 Eastbourne (i.e., according to Jarvis et al., 2006 and to Voigt et al., 2008), in order to verify which
351 option provides the highest correlation coefficient of the best-fit regression line. Depth of events
352 used to constrain the graphic correlations and their source are listed in Table 3. For the Pueblo
353 section, we considered the youngest record for extinctions and the oldest record for appearances in
354 case the same event was recognized in different positions by different authors, with the exception of
355 the HO of *R. cushmani*, which is according to Leckie (1985).
356
357 *6.1.1. Pueblo* vs. *Eastbourne*
358 The graphic correlation shows that the LO of *H. praehelvetica* is delayed at Pueblo or fall in an
359 earlier stratigraphic interval at Eastbourne, therefore this event was excluded from the calculation of
360 the regression line (Fig. 8a). We also excluded the HO of *Th. greenhornensis*, because this event
361 falls in between peaks A and B of the $\delta^{13}C$ curve at Pueblo and below peak A at Eastbourne, thus is
362 delayed in the former section.
363 The values of the correlation coefficient of the regression line (R^2) calculated using all the other
364 common events identified at Pueblo and at Eastbourne are similar when considering peak C placed
365 according to Jarvis et al. (2006) (R^2=0.90849) and according to Voigt et al. (2008) (R^2=0.92105).
366 However, the graphic correlation highlights a possible variation in the sedimentation rate in one or

367 both sections from around peak B, as testified by a change in the inclination of the line joining the
368 events in the upper right of Fig. 8a. A significant decrease in the sedimentation rate in the upper part
369 of the Eastbourne section is in agreement with the age model developed by Keller et al. (2001) and
370 is likely due to a drop in the terrigenous input starting from the transition between the Plenus Marls
371 Member (deposited during a sea-level low-stand) and the White Chalk Formation (deposited during
372 a high-stand). A slight decrease in the sedimentation rate was also identified at Pueblo
373 approximately at the same stratigraphic level (near the base of the ammonite *Neocardioceras juddii*
374 Zone) (Meyers et al., 2001) in agreement with the age-depth model build in this study. Based on the
375 observations above, we calculated two regression lines as follows: (1) from the base of the sections
376 to the HO of "*G.*" *bentonensis* and (2) from peak B to the top of the sections, both having a
377 correlation coefficient significantly high (R^2= 0.97 and R^2=0.96, respectively) (Fig. 8a). In the latter
378 case, we used the position of peak C as identified by Voigt et al. (2008), because it falls much closer
379 to the other events and we maintained this interpretation in the discussion below.
380
381 *6.1.2. Pueblo vs. Tarfaya*
382 The graphic correlation highlights many differences in the position of the events (Fig. 8b). Firstly,
383 the $\delta^{13}C$ peaks are not perfectly aligned, suggesting a decrease in the sedimentation rate from peak
384 B to peak C at Pueblo or an increase at Tarfaya, and/or an erroneous interpretation of their position
385 on the $\delta^{13}C_{org}$ profile that may have been affected by diagenetic alteration as observed for the
386 $\delta^{13}C_{carb}$ record (Tsikos et al., 2004). The presence of a 3-m thick coring gap and only two common
387 events in the upper part of the sections, including the LO of *Q. gartneri* that likely falls within the
388 non-recovery interval, complicate its interpretation (Fig. 8b).

389 Discrepancies are also found in the planktonic foraminiferal and calcareous nannofossil data, and
390 the only events that appear trustable for correlation between Pueblo and Tarfaya are the LO of *H.*
391 *praehelvetica* and the extinctions of *Th. deeckei* and *Th. greenhornensis*, as well as the onset of the
392 "*Heterohelix*" shift. By contrast, the HO of *A. albianus* is delayed at Pueblo or falls in an earlier
393 stratigraphic interval at Tarfaya, while the opposite is true for the HO of *R. cushmani* and of "*G."*
394 *bentonensis*. These three events were not used to calculate the regression line, as they might be
395 diachronous between the two sections. Although we do not observe any sedimentological or
396 stratigraphic evidence of interruption of sedimentation, an alternative explanation to the apparently
397 delayed extinctions of *R. cushmani* and of "*G." bentonensis* at core S57 invokes the presence of a
398 short hiatus between the HO of "*G." bentonensis* and the onset of the "*Heterohelix*" shift, that
399 would explain why these events are stratigraphically closer in this section compared to Pueblo and
400 would move down the HO of *R. cushmani* and "*G." bentonensis* to the correlation line. Moreover, a
401 short hiatus in this position would complicate the interpretation of peaks A and B of the $\delta^{13}C_{org}$
402 profile adding further uncertainties to the correlation between Pueblo and Tarfaya. Because of the
403 uncertainties regarding the position of the $\delta^{13}C$ peaks and little number of common events at the top
404 of the stratigraphic interval studied, the evaluation of the reliability of planktonic foraminiferal
405 events for correlation between Pueblo and Tarfaya requires further study and comparison with
406 sections elsewhere.
407
408 *6.3. Testing the accuracy of mid-low latitude correlations using planktonic foraminifera*
409 In order to compare all the sections available and with the attempt to test the reliability of bioevents
410 for correlating mid-low latitudes localities, we used the $\delta^{13}C$ isotope excursion, assuming that it was
411 synchronously registered in the sedimentary successions. We have plotted in Fig. 9 the planktonic

foraminiferal bioevents herein identified at Eastbourne and Tarfaya and those documented from the selected stratigraphic sections (Pueblo, Clot Chevalier, Pont d'Issole, wadi Bahloul and Gongzha) against a schematic $\delta^{13}C$ profile. The LO of *H. helvetica* at Pueblo is plotted in Fig. 9 according to all authors. A summary of the most reliable sequence of planktonic foraminiferal bioevents resulting from our study is reproduced in Fig. 10.

6.3.1 Reliability of zonal markers

The extinction of *R. cushmani* at Pueblo is recorded in slightly different stratigraphic intervals: from slightly below A to in between A and B of the $\delta^{13}C$ curve. However, robust data based on both thin sections and washed residues place the HO of *R. cushmani* in the trough of $\delta^{13}C$ values above peak A in the $\delta^{13}C$ curve (Table 1; Leckie, 1985; Leckie et al., 1998; Caron et al., 2006; Elderbak and Leckie, 2016). Remarkable is the identification of atypical *R. cushmani* up to peak C (Leckie, 1985; Desmares et al., 2007), representing the youngest record of morphotypes falling within the range of variability of *R. cushmani* documented in the literature (Fig. 9). The HO of *R. cushmani* is diachronous from south to north within the WIS (Leckie, 1985; Desmares et al., 2007; Lowery et al., 2014), which is not surprising because of the local variations in the salinity, sea-surface temperatures and productivity, and the relatively shallow water depth (e.g., Caldwell and Kauffman, 1993; Arthur et al., 1985; Pratt, 1984, 1985; Leckie, 1985; Leckie et al., 1998; Pagani and Arthur, 1998; West et al., 1998; Keller et al., 2004; Corbett and Watkins, 2013; Lowery et al., 2014; Elderbak et al., 2014; Elderbak and Leckie, 2016, among many others) that might have hindered the migration of pelagic organisms throughout the basin.

In the other sections examined, the HO of *R. cushmani* is typically recorded in between peak A and B, with the exception of Clot Chevalier and Tarfaya. In the former section, this event falls in

435 an earlier stratigraphic interval (below A) due to a combination of causes: (1) the presence of hiatus
436 at the base of the Thomel Level and of an overlying condensed stratigraphic interval, and (2) the
437 rarity of *R. cushmani* toward the top of its stratigraphic range, so that a possible hiatus or low
438 sedimentation rate in this interval might considerably bias the position of its HO (Falzoni et al.,
439 2016b). A more reliable HO of *R. cushmani* in the Vocontian Basin is identified at Pont d'Issole in
440 between A and B (Grosheny et al., 2006; Grosheny et al., 2017).
441 The extinction of *R. cushmani* is recorded at Tarfaya (core S57) a few cm above the
442 supposed peak B, while it falls at peak B in other cores drilled in the Tarfaya Basin (core S75:
443 Kuhnt et al., 2005). Because of the remarkable similarity of these Moroccan core sections, and in
444 the absence of sedimentological and micropaleontological evidences supporting reworking of older
445 sediments at core S57, the extinction of *R. cushmani* appear to be slightly delayed in this area of the
446 central Atlantic Ocean, as testified by the graphic correlation between Tarfaya and Pueblo.
447 However, confirming the delayed HO of *R. cushmani* in this locality requires further studies,
448 because of the potentially diagenetically altered $\delta^{13}C_{org}$ record of core S57 and the possible presence
449 of intervals of interruption of sedimentation.
450 The appearance of *H. helvetica* is recorded across a 3 m-thick stratigraphic interval at
451 Pueblo (Fig. 2) corresponding to the interval from slightly above peak C to the point where the
452 $\delta^{13}C_{carb}$ returns to pre-excursion values (Fig. 9). The appearance of *H. helvetica* at Pont d'Issole and
453 Gongzha falls slightly above point C, in agreement with its oldest identifications at Pueblo.
454 According to Tsikos et al. (2004) and in this study, *H. helvetica* does not occur at Eastbourne and at
455 Tarfaya, and it is not identified at Clot Chevalier (Falzoni et al., 2016b). Our study confirms the
456 unreliability of the LO of *H. helvetica* as a marker event for the base of the Turonian, as explained
457 in the Introduction section.

458

459 *6.4. Secondary planktonic foraminiferal bioevents for mid-to-low latitude correlations*

460 *6.4.1. Reliable bioevents*

461 Extinctions across the C–T boundary interval follow a well-defined scheme that is reproducible in
462 all the stratigraphic sections examined, as listed below in stratigraphic order: 1) HO of *Th. deeckei*,
463 2) HO of *Th. greenhornensis*, overlaid by the HO of *R. cushmani*, and by 3) the HO of *"G".*
464 *bentonensis* (Figs. 9-10).

465 1) The extinction of *Th. deeckei* always falls below peak A on the $\delta^{13}C$ curve, approximately around
466 the point where the $\delta^{13}C$ profile begins to increase (Clot Chevalier, Pont d'Issole and Gongzha) or
467 in a slightly younger stratigraphic interval where the $\delta^{13}C$ profile changes its grade and increases
468 more distinctly (Pueblo, Eastbourne, Tarfaya).

469 2) The HO of *Th. greenhornensis* falls slightly below or at peak A, with the exception of Pueblo,
470 where it falls in between A and B and together with the HO of *R. cushmani*, suggesting a
471 significantly delayed extinction in the WIS compared to the other mid-low latitude localities.
472 Limited discrepancies in the HO of *Th. greenhornensis* and *Th. deeckei* might be related to
473 differences in sampling resolution and/or rareness of both species towards the top of their
474 stratigraphic distribution. In other localities, the extinction of both species is recorded in the
475 uppermost *R. cushmani* Zone (Blake Nose Plateau: Huber et al., 1999; Austria: Gebhardt et al.,
476 2010; Switzerland: Westermann et al., 2010), with the exception of an apparently earlier HO of *Th.*
477 *deeckei* in Tunisia (Robaszynski et al., 1993) and Japan (Hasegawa, 1999) and of *Th.*
478 *greenhornensis* in Morocco (Keller et al., 2008). It is worth mentioning that different *Th. deeckei*
479 species concepts might have been applied in the literature. For instance, Pessagno (1967) retained

480 *Th. deeckei* a possible junior synonym of *Th. greenhornensis*, while it has been identified as distinct
481 species by subsequent authors (e.g., Robaszynski et al., 1979; Ando and Huber, 2007).
482 3) The extinction of *"G". bentonensis* is recorded either slightly below (Pueblo, Eastbourne
483 and Clot Chevalier) or immediately above the supposed peak B (Tarfaya). Because this species was
484 not identified at wadi Bahloul and Gongzha, its extinction level in the eastern Tethyan realm cannot
485 be assessed. Based on the available data and pending further biostratigraphic studies in sections
486 belonging to this paleogeographic area, the HO of *"G". bentonensis* appears a very reliable marker
487 for the latest Cenomanian. Its apparently slightly delayed extinction at Tarfaya should be verified
488 by further studies (see discussion in paragraph 6.3.1 regarding the HO of *R. cushmani*). Further
489 support to its validity is provided by its identification always some centimeters to few meters above
490 the extinction of *R. cushmani* in Spain (Lamolda et al., 1997) and Morocco (Keller et al., 2008),
491 while the apparently synchronous extinction of the single-keeled rotaliporids and of *"G".*
492 *bentonensis* in several Italian sections (Bottaccione-Contessa: Premoli Silva and Sliter, 1995,
493 Coccioni and Premoli Silva, 2015; Antruiles, Dolomites: Luciani and Cobianchi, 1999; Calabianca-
494 Guidaloca: Scopelliti et al., 2004; Valdagno: Coccioni and Luciani, 2005) is due to the absence of
495 planktonic foraminifera in the C_{org}-enriched layers of the Bonarelli Level (or equivalent) and/or to
496 the stratigraphic gap across the C/T boundary (Gambacorta et al., 2015).
497 In addition, the LOs of *D. hagni* and *D. imbricata* that are usually recognized below the
498 beginning of the $\delta^{13}C$ isotopic excursion, also appear reliable for correlation as discussed below
499 (Figs. 9-10):
500 4) The LO of *D. hagni* is recorded from the base of the sections in most of the localities
501 examined, with the exception of Pont d'Issole (i.e., across the $\delta^{13}C$ rise below A) and wadi Bahloul
502 (i.e., slightly above B). However, its appearance level is well documented in the mid-to-upper *R.*

503 *cushmani* Zone of other geographic localities including Tunisia (Robaszynski et al., 1993),
504 Morocco (Keller et al. 2008), Italy (Premoli Silva and Sliter, 1995; Luciani and Cobianchi, 1999;
505 Mort et al., 2007; Coccioni and Premoli Silva, 2015), Spain (Lamolda et al., 1997), Austria
506 (Gebhardt et al., 2010), Switzerland (Westermann et al., 2010), Blake Nose Plateau (Huber et al.,
507 1999), and Japan (Hasegawa, 1999). We believe that its delayed occurrence at Pont d'Issole and
508 wadi Bahloul might rely on its rarity in these localities and/or availability of small-sized samples.
509 This latter hypothesis is supported by the fact that planktonic foraminifera from Pont d'Issole and
510 wadi Bahloul were studied in thin sections in layers characterized by a particularly indurated
511 lithology. Thin sections represent a smaller sized sample compared to washed residues and their
512 study reduces the likelihood of encountering rare species. Discrepancies in the LO of *D. hagni* at
513 low latitudes are found in the WIS: at Pueblo, the LO of *D. hagni* is at the extinction level of
514 rotaliporids (Leckie, 1985), while in south Texas, the LO lies above the extinction level of
515 rotaliporids (Frush and Eicher, 1975; Lowery and Leckie, 2017) suggesting an ecologic control at
516 the southern aperture of the WIS relative to sites to the north in the core of the seaway (recorded as
517 *P. difformis*, Eicher and Worstell, 1970; Eicher and Diner, 1985), indicating that the LO of this
518 species is likely diachronous for sections within the WIS. This diachronous pattern in the WIS is
519 similar to that of the HO of *R. cushmani*, which is also from south to north (Leckie, 1985).
520 5) The LO of *D. imbricata* is identified from the base of the sections or in the lowermost
521 samples at Pueblo, Eastbourne, Tarfaya, and Clot Chevalier. Its LO appears delayed in the sections
522 that have been partially studied in thin section as follows: at Pont d'Issole (close to excursion A), at
523 Gongzha (slightly above excursion B), and at wadi Bahloul (in between B and C). In sections
524 elsewhere, its LO is documented in the *R. cushmani* Zone (Italy: Premoli Silva and Sliter, 1995;
525 Luciani and Cobianchi, 1999; Coccioni and Luciani, 2004; Mort et al., 2007; Coccioni and Premoli

Silva, 2015; Spain: Lamolda et al., 1997; Japan: Hasegawa, 1999; Morocco: Keller et al., 2008) and in the *W. archaeocretacea* Zone (Austria: Gebhardt et al., 2010; Switzerland: Westermann et al., 2010). Despite some discrepancies in the LO of *D. imbricata* might be related to subjective species concepts, we believe that its apparent diachronism might rely on the sample size, as this species is often uncommon at the beginning of its stratigraphic range. Overall, in our opinion the appearance of *D. imbricata* can be considered a trustable bioevent for correlation in cases where the size of the samples studied is large enough to encounter rare species.

6.4.2. Bioevents potentially useful but requiring further investigations

1) The LO of *P. algeriana* is an upper Cenomanian event falling in the mid-upper *R. cushmani* Zone below the $\delta^{13}C$ isotope excursion A (Pueblo, Pont d'Issole, wadi Bahloul), whereas the occurrence of this species is recorded at Eastbourne, Tarfaya, Clot Chevalier and Gongzha from the base of the section, so that its LO cannot be precisely determined (Fig. 9). However, the appearance of *P. algeriana* is documented in the lower *R. cushmani* Zone (Italy: Premoli Silva and Sliter, 1995; Luciani and Cobianchi, 1999; Spain: Lamolda et al., 1997; Blake Nose Plateau: Huber et al., 1999). Accordingly, several authors identified a *P. algeriana* Subzone defined as the stratigraphic interval between the LO of *P. algeriana* and the HO of *R. cushmani* (Bottaccione-Contessa: Premoli Silva and Sliter, 1995; Coccioni and Premoli Silva, 2015; Eastbourne: Keller et al., 2001). This diachronous appearance likely reflects different species concepts among authors as testified by its accommodation either in the genus *Praeglobotruncana* (Caron, 1966) or *Dicarinella* (Robaszynski et al., 1979). Recently, its distinctive morphological features have been clarified to promote its identification and calibrate its appearance level at a regional to global scale (see Falzoni et al., 2016b).

549 2) The occurrence of *P. oraviensis* is rarely recorded in the literature with few exceptions (Tunisia:
550 Robaszynski et al., 1990; Spain: Lamolda et al., 1997; Crimea: Kopaevich and Vishnevskaya, 2016;
551 Clot Chevalier: Falzoni et al., 2016b) and its species concept has been differently interpreted by
552 authors including its generic attribution, because of the unavailability of SEM images of the type
553 material (see Falzoni et al., 2016b for taxonomic details). Possibly because of these taxonomic
554 uncertainties, the appearance of *P. oraviensis* is recorded in different levels within the *W.*
555 *archaeocretacea* Zone (Robaszynski et al., 1990; Lamolda et al., 1997; Kopaevich and
556 Vishnevskaya, 2016; Falzoni et al., 2016b). At Eastbourne, we identify the LO of *P. oraviensis* at
557 the top of *R. cushmani* Zone, representing the oldest record of this species documented in the
558 literature (Figs. 9-10). The delayed occurrence of *P. oraviensis* at Clot Chevalier, in the middle-
559 upper *W. archaeocretacea* Zone likely results from a combination of sedimentologic (hiatus and
560 condensed stratigraphic interval at the top of the *R. cushmani* Zone) and ecologically-related (very
561 rare occurrence of planktonic foraminifera within the lower *W. archaeocretacea* Zone) causes.
562 *Praeglobotruncana oraviensis* does not occur at Tarfaya or at Pueblo, suggesting that some
563 ecologic features (e.g., water depth, trophic regime) might have controlled its geographic
564 distribution at least at the beginning of its stratigraphic range, therefore the reliability of its LO
565 requires further investigation and calibration with other sections.
566 2) The LO of *M. schneegansi* is recorded slightly above peak C at Pont d'Issole (Grosheny
567 et al., 2006), while ancestor morphotypes named *M.* cf. *schneegansi* do occur at Clot Chevalier in a
568 slightly younger stratigraphic interval where $\delta^{13}C$ returns close to pre-excursion values (Falzoni et
569 al., 2016b) (Fig. 9). The LO of *M. schneegansi* is identified in sediments of approximately coeval
570 age either slightly below (Japan: Hasegawa, 1999) or above the LO *H. helvetica* (Tunisia:
571 Robaszynski et al., 1990; Italy: Premoli Silva and Sliter, 1995; Coccioni and Premoli Silva, 2015;

572 Texas: Lowery and Leckie, 2017). Unfortunately, the synchronicity of the appearance of *M.*
573 *schneegansi* in these sections cannot be accurately tested, lacking the $\delta^{13}C$ profile. In addition, *M.*
574 *schneegansi* is not documented in the lowermost Turonian of the other localities examined and it is
575 absent in the southern mid-high latitudes (Petrizzo, 2000, 2001), suggesting that its geographic
576 distribution might be confined to the tropical-subtropical latitudinal bands. Consequently, the
577 reliability of its LO requires further study, but it might represent a useful bioevent falling close to
578 the C/T boundary at least at low latitudes (Fig. 10).
579 3) The LO of *M. sigali* is detected well above peak C, but within the lower *H. helvetica*
580 Zone, at Pueblo and at Gongzha, although it seems to be delayed in the former section. Possible
581 ancestor morphotypes of *M. sigali* do occur at Clot Chevalier approximately across the same
582 stratigraphic interval (above C) (Fig. 9). This species is absent at Tarfaya, Eastbourne, Pont
583 d'Issole, and wadi Bahloul, but it is usually documented to first occur slightly below (Furlo: Mort et
584 al., 2007; south Texas: Lowery and Leckie, 2017), or above the LO of *H. helvetica* (Tunisia:
585 Robaszynski et al., 1990; Italy: Premoli Silva and Sliter, 1995; Coccioni and Premoli Silva, 2015;
586 Switzerland: Westermann et al., 2010). Because the appearance level of *M. sigali* is still not
587 documented in several localities, its reliability for mid-to-low latitude correlation requires further
588 studies.
589 4) LO of other *Marginotruncana* species. The LO of *M. renzi* was identified well above C at
590 the top of the Eastbourne section by Paul et al. (1999) in a slightly younger stratigraphic interval
591 compared to that here re-studied and assigned to the ammonite *Mammites nodosoides* Zone (Figs. 3
592 and 9). The LO of *M. renzi* is documented slightly above the LO of *H. helvetica* at the Blake Nose
593 Plateau (Huber et al., 1999), in south Texas (Lowery and Leckie, 2017), Italy (Premoli Silva and
594 Sliter, 1995; Coccioni and Premoli Silva, 2015), and Tunisia (Robaszynski et al., 1990). The LO of

595 *M. marianosi* is documented at Pueblo and Pont d'Issole falling in the *H. helvetica* Zone and above
596 C, where the $\delta^{13}C$ returns close to pre-excursion values, respectively (Fig. 9). In other localities, the
597 LO of *M. marianosi* is recorded below (Furlo: Mort et al., 2007) or slightly above (Bottaccione-
598 Contessa: Premoli Silva and Sliter, 1995) the LO of *H. helvetica*, but this bioevent is significantly
599 delayed in the southern mid-latitudes (Exmouth Plateau: Petrizzo, 2000), as it falls above the
600 extinction of *Falsotruncana maslakovae* in the late Turonian-early Coniacian. The LO of *M.*
601 *coronata* is identified in the lower (Pont d'Issole: Grosheny et al., 2006) or at the top of the *H.*
602 *helvetica* Zone in the Tethyan Realm (Tunisia: Robaszynski et al., 1990; Italy: Premoli Silva and
603 Sliter, 1995; Coccioni and Premoli Silva, 2015; Tanzania: Huber and Petrizzo, 2014), and in the
604 southern mid-latitudes (Exmouth Plateau: Petrizzo, 2000). In south Texas, the LO of *M. coronata* is
605 above the HO of *H. helvetica* (Frush and Eicher, 1975; Lowery and Leckie, 2017).
606 Overall, the reliability for correlation of *Marginotruncana* species needs further
607 investigations and calibration with the carbon isotope record in other localities. Noteworthy, the
608 appearance of marginotruncanids predates the LO of *H. helvetica* in the southern Indian Ocean
609 (Kerguelen Plateau: Petrizzo, 2001), potentially representing a powerful tool to correlate low-to-
610 high latitude records.
611
612 *6.4.3. Misleading bioevents*
613 1) The LO of *H. praehelvetica* has been recorded from below peak A (well below the beginning of
614 the $\delta^{13}C$ isotopic excursion) to below peak B (Fig. 9) and in different stratigraphic levels at Pueblo
615 and Eastbourne (Figs. 2-3). This bioevent is identified in the literature, either in the *R. cushmani*
616 Zone (Bottaccione: Premoli Silva and Sliter, 1995; Furlo: Mort et al., 2007; Antruiles, Dolomites:
617 Luciani and Cobianchi, 1999; Blake Nose Plateau: Huber et al., 1999; Tarfaya: Keller et al., 2008),

618 at the extinction level of the rotaliporids (Leckie, 1985), or within the lower *W. archaeocretacea*
619 Zone (Tunisia: Robaszynski et al., 1990; Spain: Lamolda et al., 1997). These discrepancies are
620 likely due to the common occurrence of transitional morphotypes between *H. praehelvetica* and its
621 ancestor *Whiteinella aprica* making the identification of the first representative of the species
622 almost subjective (Huber and Petrizzo, 2014). Because of the observations listed above, we regard
623 the LO of *H. praehelvetica* as an unreliable marker for correlation.
624 2) *Whiteinella archaeocretacea* occurs from the base (or nearly the base) of the section at
625 Pueblo, Eastbourne, Gongzha and wadi Bahloul, while its LO is recorded slightly below A at Pont
626 d'Issole. Specimens strictly resembling the holotype were not identified at Tarfaya and Clot
627 Chevalier (Fig. 9). At Eastbourne, *W. archaeocretacea* is extremely rare and shows a very
628 discontinuous stratigraphic distribution, suggesting that the identification of its lowest appearance
629 level might be strongly biased by a low sampling resolution or by the analyses of small-sized
630 samples. Discrepancies in its LO might also be due to a subjective species concept, because
631 specimens having a rounded (resembling the holotype) as well as a pinched lateral profile
632 (resembling the paratype) were retained to fall in its range of variability. Pending further taxonomic
633 studies and because of its rarity in the assemblages, we regard the LO of *W. archaeocretacea* as an
634 unreliable bioevent.
635 3) The extinctions of *R. montsalvensis* and *Th. brotzeni* have been identified at Gongzha
636 well below the $\delta^{13}C$ excursion. At Eastbourne *Th. brotzeni* disappears in the stratigraphic interval
637 where we observe the first $\delta^{13}C$ rise, while *R. montsalvensis* becomes extinct slightly above the
638 beginning of the second $\delta^{13}C$ rise, both below A (Fig. 9). Both bioevents have been recorded to fall
639 in the middle *R. cushmani* Zone in the Bottaccione-Contessa composite section (Coccioni and
640 Premoli Silva, 2015), where *R. montsalvensis* and *Th. brotzeni* show a scattered occurrence toward

641 the top of their stratigraphic range (as well as at Eastbourne), leading to some uncertainties
642 regarding the position of their extinction level. By contrast, other studies indicate the HO of both
643 species falls in an older stratigraphic interval below the appearance of *R. cushmani* (Hasegawa,
644 1999; Westermann et al., 2010). Pending further studies, we interpret the HO of *R. montsalvensis*
645 and *Th. brotzeni* as being controlled by local environmental conditions and because of their rarity
646 toward the top of their stratigraphic distribution we discourage to use their extinction level for
647 correlation.

648 4) The LO of *D. elata* is recorded below excursion A (Pueblo, Clot Chevalier, Eastbourne)
649 and above excursion B (wadi Bahloul and Gongzha) (Fig. 9). Remarkably, *D. elata* is identified co-
650 occuring with *Thalmanninella globotruncanoides* in the middle Cenomanian of Tunisia (Kalaat
651 Senan: Robaszynski et al., 1993), representing its oldest documented record in the literature. Most
652 studies identified its LO in the uppermost *R. cushmani* Zone in Spain (Lamolda et al., 1997),
653 whereas its occurrence is not recognized at Tarfaya and Pont d'Issole, in the Italian sections
654 (Bottaccione section: Premoli Silva and Sliter, 1995; Coccioni and Luciani, 2004; Coccioni and
655 Premoli Silva, 2015; Antruiles, Dolomites: Luciani and Cobianchi, 1999; Furlo: Mort et al., 2007),
656 at the Blake Nose Plateau (Huber et al., 1999), in Morocco (Keller et a., 2008), Switzerland
657 (Westermann et al., 2010) and Japan (Hasegawa, 1999). Although discrepancies in its LO might be
658 related to the rarity of *D. elata* in some environmental settings, so that its occurrence might not be
659 detected in small-sized samples and poorly resolved biostratigraphic studies, the observations listed
660 above support its unreliability for correlation, because of its presumably stenotopic ecology and
661 absence in several localities. Discrepancies in the identification of its appearance level may also
662 relay on different species concepts.

5) The LO of *D. canaliculata* has been recorded to fall in different stratigraphic levels as follows: below the initial $\delta^{13}C$ positive excursion (Pueblo and Eastbourne), slightly below excursion A (Clot Chevalier), above excursion C (Pont d'Issole and wadi Bahloul), whereas *D. canaliculata* is absent at Tarfaya and Gongzha (Fig. 9). Discrepancies in its appearance level are found in other localities: its LO is identified in the upper *R. cushmani* Zone (Bottaccione-Contessa: Coccioni and Premoli Silva, 2015; Antruiles, Dolomites: Luciani and Cobianchi, 1999; Japan: Hasegawa, 1999), within the *W. archaeocretacea* Zone (Blake Nose Plateau: Huber et al., 1999), and within the *H. helvetica* Zone (Tunisia: Robaszynski et al., 1990). The sections in south Texas may have experienced conditions of environmental exclusion, very low abundances, and/or poor preservation that result in a much delayed LO of *D. canaliculata* within or at the top of the *H. helvetica* Zone (Lowery and Leckie, 2017). Based on the above and on its distinctive morphology, we interpret this bioevent to be considerably diachronous and likely subject to ecologic control.

6) The genus *Anaticinella* was erected to include ecophenotypes that evolved from the typical single-keeled rotaliporids by losing the peripheral keel and inflating the chambers on both the umbilical and spiral sides (Eicher, 1973); this morphologic adaptation was interpreted as forced by the expansion of the oxygen minimum zone at the onset of the OAE 2 that induced the exploitation of sea-surface habitats by taxa that were deep-dwellers (Wonders, 1980; Leckie, 1985; Desmares et al., 2007). Two species were included in the genus *Anaticinella* (=*Pseudoticinella* Longoria, 1973): *multiloculata* and *planoconvexa* (Longoria, 1973). More recently, *planoconvexa* was accommodated in the genus *Rotalipora*, as it was interpreted to directly evolve from *R. cushmani* (Desmares et al., 2008), while the species *multiloculata* belongs to the *Th. greenhornensis* phyletic lineage, thus was accommodated in the genus *Thalmanninella* (González Donoso et al., 2007; Desmares et al., 2008). *Anaticinella* species have been largely documented in the WIS

686 (Morrow, 1934; Eicher and Worstell, 1970; Eicher, 1973; Leckie, 1985; Keller and Pardo, 2004;
687 Caron et al., 2006; Desmares et al., 2007; 2008), but their occurrence is also recorded in other low
688 latitudes localities (Eastbourne: Keller et al., 2001; France: Grosheny et al., 2006; Tunisia: Caron et
689 al., 2006; Grosheny et al., 2013; Morocco: Keller et al., 2008; Tibet: Bomou et al., 2013).
690 Desmares et al. (2007) identified the extinction of *Th. multiloculata* and *R. planoconvexa* at
691 Pueblo as follows: a) HO *Th. multiloculata* in between excursions A and B, and b) HO *R.*
692 *planoconvexa* slightly above excursion C (Fig. 9). The HO of *Th. multiloculata* is recorded below A
693 at Pont d'Issole (Grosheny et al., 2006) and close to A at Gongzha (Bomou et al., 2013), while the
694 HO of *Anaticinella* species is recorded slightly above C at wadi Bahloul. Morphotypes falling in the
695 range of variability of *Th. multiloculata* and *R. planoconvexa* are not identified at Clot Chevalier
696 (Falzoni et al., 2016b) and neither at Eastbourne and Tarfaya, although *Th. multiloculata* is
697 recognized at Eastbourne by Keller et al. (2001). Specimens resembling *R. cushmani* but having 4
698 to 5 chambers more inflated chambers and a very weakly developed peripheral keel on the first
699 chambers of the last whorl occur rarely at Eastbourne (here figured in Fig. 5, 2a–c). In our opinion
700 and according to Robaszynski et al. (1993), these specimens closely resemble to the original
701 description and to the drawing of the holotype of *Rotalipora praemontsalvensis* (Ion, 1976), rather
702 than to *R. planoconvexa* (Longoria, 1973). However, such specimens might have been included in
703 the genus *Anaticinella* or in the atypical *R. cushmani* morphotypes by previous authors (e.g.,
704 Leckie, 1985; Caron et al., 2006; Desmares et al., 2007), especially when observed in thin sections.
705 Further studies are required to better assess the taxonomic status and phyletic relationship among
706 rotaliporids. On the other hand, the geographic distribution of *Th. multiloculata* and of *R.*
707 *planoconvexa* (sensu stricto) should be further investigated and their occurrence outside the WIS

708 should be more robustly supported. However, the extinction of *Anaticinella* species is clearly
709 diachronous (Fig. 9).
710 7) The "*Heterohelix* shift" was first described by Leckie (1985), Leckie et al. (1998), and
711 West et al. (1998) in the WIS as an abrupt change planktonic foraminiferal assemblages, which
712 became dominated by biserial taxa (>50% of the population). Accordingly, it has been interpreted
713 as a period of unstable eutrophic surface water conditions that inhibited the proliferation of the
714 keeled K-strategist taxa. The "*Heterohelix* shift" is identified below excursion A at Gongzha,
715 between excursions A and B at wadi Bahloul, and between excursions B and C at Pueblo and
716 Tarfaya (Fig. 9). The "*Heterohelix* shift" is not documented in the Vocontian Basin (Clot Chevalier,
717 Pont d'Issole), but recognized around excursion B at Eastbourne (Keller et al., 2001) as an increase
718 in the abundance of biserial taxa from 40% to >60% of the population in the >63 μm size-fraction.
719 Such a dominance of heterohelicids could not be confirmed in the samples examined during this
720 study that instead revealed an increase in the abundance of calcispheres in the same stratigraphic
721 interval (Fig. 11), as reported by Pearce et al. (2009). The "*Heterohelix* shift" is documented in the
722 lower-middle *W. archaeocretacea* Zone of other localities (Italy: Coccioni and Luciani, 2004;
723 Tunisia: Nederbragt and Fiorentino, 1999; Morocco: Keller et al. 2008), with the exception of
724 Huber et al. (1999), who identified this bioevent in the lower *H. helvetica* Zone at the Blake Nose
725 Plateau. Despite the onset of the "*Heterohelix* shift" is apparently synchronous between Pueblo and
726 Tarfaya (Fig. 8b), its diachronous occurrence across the other mid-low latitude localities (Fig. 9)
727 discourages its application for interbasinal correlations.
728
729
730 **7. Conclusion**

A highly-resolved biostratigraphic analysis of planktonic foraminiferal assemblages at Eastbourne and Tarfaya, compared with the record at the Turonian GSSP in Colorado, allowed recognition of a sequence of bioevents that are compared to those recorded in other sections available in the literature and correlated to the $\delta^{13}C$ profile. We calculated reliable estimates of the age of most planktonic foraminiferal events identified in the Pueblo GSSP section, including the extinction of the zonal marker *R. cushmani*. Results of graphic correlations and comparison between the sections analyzed indicate that the extinctions of Cenomanian taxa represent the most reproducible sequence of bioevents at mid-low latitudes and should be considered reliable for supra-basinal correlations. This sequence includes, in stratigraphic order, the HOs of: (1) *Th. deeckei*, (2) *Th. greenhornensis*, (3) *R. cushmani*, and (4) *"G". bentonensis*. Few exceptions to this scheme are detected at Pueblo (delayed HO of *Th. greenhornensis*) and at Tarfaya (delayed HO of *R. cushmani* and of "*G.* *bentonensis*) (Fig. 10). Also, the extinction of *R. cushmani* is diachronous within areas of the WIS. The LOs of *D. hagni* and *D. imbricata* in the pre-excursion interval may be considered additional trustable bioevents for correlation in case the size of the samples used for planktonic foraminiferal biostratigraphy is large enough to ensure the identification of rare species.

Additional useful bioevents that, however, require further investigation, because of their rare identification in several localities or poor calibration with other bio- and chemostratigraphic data are the LOs of *Praeglobotruncana oraviensis* at the top of the *R. cushmani* Zone, and of *Marginotruncana schneegansi,* the latter being particularly promising to approximate the C/T boundary in low latitudes localities. Little information is presently available to test the synchronicity of the appearance of *P. algeriana* in the mid-upper Cenomanian and of other *Marginotruncana* species (i.e, *M. sigali*, *M. coronata* and *M. marianosi*), in the Turonian, but these

754 events appear worth of being further investigated. By contrast, the geographic and stratigraphic
755 distribution of *D. elata*, and *D. canaliculata* were likely ecologically driven; however,
756 inconsistencies in the application of different species concepts by authors are difficult to assess, but
757 might have introduced additional discrepancies in the identification of their LOs. A very transitional
758 evolution from the ancestor species and different species concepts among authors can be invoked as
759 a cause for the diachronous LO of *H. praehelvetica* and *H. helvetica*, while *W. archaeocretacea*, *Th.*
760 *brotzeni* and *R. montsalvensis* occur too rarely in the stratigraphic interval examined, so that their
761 appearance/extinction can be misleading to trace correlations. Finally, our study confirms the
762 unreliability of the LO of *H. helvetica* as a marker for the base of the Turonian and suggests that the
763 "*Heterohelix* shift" represents a response of the planktonic foraminiferal assemblages to a
764 local/regional increase in sea-surface productivity. In addition, we highlight that the occurrence of
765 anaticinellids (sensu strictu) is still poorly documented outside the WIS and, regardless, their
766 extinctions are clearly diachronous.
767 To conclude, we remark that further efforts have still to be directed toward the stabilization
768 of the taxonomic concepts of several planktonic foraminiferal species, in order to assure an univocal
769 approach during biostratigraphic analyses. Moreover, a small sample size and/or a low sampling
770 resolution might significantly influence the level at which LO and HO are identified even in case
771 the bioevent is geologically isochronous and these factors should be taken in consideration when
772 tracing correlations. On the other hand, we underline that the identification of the $\delta^{13}C$ peaks and
773 troughs is not straightforward and should always be supported by a highly-resolved sequence of
774 bioevents.
775
776 **Acknowledgements**

Agostino Rizzi (CNR, Italy) is thanked for assistance at the SEM. FF carried out this research during a post-doc fellowship of the University of Milan. This study was funded by MIUR-PRIN 2010-2011 (2010X3PP8J_001) to Elisabetta Erba (scientific coordinator).

References

Ando, A., Huber, B.T., 2007. Taxonomic revision of the late Cenomanian planktonic foraminifera *Rotalipora greenhornensis* (Morrow, 1934). Journal of Foraminiferal Research 37, 160–174.

Anthonissen, D.E., Ogg, J.G., 2012. Appendix 3: Cenozoic and Cretaceous biochronology of planktonic foraminifera and calcareous nannofossils. The geologic time scale 2012, 1083–1127.

Arthur, M.A., Dean, W.E, Pollastro, R., Scholle, P.A., Claypool, G.E., 1985. A comparative geochemical study of two transgression pelagic limestone units, Cretaceous Western Interior basin, U.S. In: Pratt, L.A., Kauffman, E.G., Zelt, F.B. (Eds.), Fine Grained Deposits and Biofacies of the Cretaceous Western Interior Seaway: evidence of cyclic sedimentary processes. Field Trip Guidebook, vol. 4. Society of Economic Paleontologists and Mineralogists, Tulsa, pp. 16–27.

Bomou, B., Adatte, T., Tantawy, A.A., Mort, H., Fleitmann, D., Huang, Y., Föllmi, K.B., 2013. The expression of the Cenomanian–Turonian oceanic anoxic event in Tibet. Palaeogeography, Palaeoclimatology, Palaeoecology 369, 466–481.

Bowman, A.R., Bralower, T.J., 2005. Paleoceanographic significance of high-resolution carbon isotope records across the Cenomanian–Turonian boundary in the Western Interior and New Jersey coastal plain, USA. Marine Geology 217, 305–321.

799 Caldwell, W.G.E., Kauffman, E.G., 1993. Evolution of the Western Interior basin. St. John's,
800 Geological Association of Canada Special Papers 39, 680 pp.
801 Caron, M., 1966. Globotruncanidae du Crétacé supérieur du synclinal de la Gruyère (Préalpes
802 medians, Suisse). Revue de Micropaléontologie 9, 68–93.
803 Caron, M., Dall'Agnolo, S., Accarie, H., Barrera, E., Kauffman, E.G., Amédro, F., Robaszynski, F.,
804 2006. High-resolution stratigraphy of the Cenomanian–Turonian boundary interval at Pueblo
805 (USA) and Wadi Bahloul (Tunisia): Stable isotope and bio-events correlation. Géobios 39, 171–
806 200.
807 Carter, D.J., Hart, M.B., 1977, Aspects of mid-Cretaceous stratigraphical micropalaeontology.
808 Bulletin of the British Museum of Natural History, Geological Series 29, 1–135.
809 Cobban, W.A., Scott, G.R., 1972. Stratigraphy and ammonite fauna of the Graneros Shale and
810 Greenhorn Limestone near Pueblo, Colorado (No. 645). United States Geological Survey
811 Professional Paper 645, 108 pp.
812 Coccioni, R., Luciani, V., 2004. Planktonic foraminifera and environmental changes across the
813 Bonarelli Event (OAE2, latest Cenomanian) in its type area: A high resolution study from the
814 Tethyan reference Bottaccione section (Gubbio, central Italy). Journal of Foraminiferal Research
815 34, 109–129.
816 Coccioni, R., Luciani, V., 2005. Planktonic foraminifers across the Bonarelli Event (OAE2, latest
817 Cenomanian): The Italian record. Palaeogeography, Palaeoclimatology, Palaeoecology 224,
818 167–185.
819 Coccioni, R., Premoli Silva, I., 2015. Revised Upper Albian–Maastrichtian planktonic foraminiferal
820 biostratigraphy and magneto-stratigraphy of the classical Tethyan Gubbio section (Italy).
821 Newsletters on Stratigraphy 48, 47–90.

822 Corbett, M.J., Watkins, D.K., 2013. Calcareous nannofossil paleoecology of the mid-Cretaceous
823 Western Interior Seaway and evidence of oligotrophic surface waters during OAE2.
824 Palaeogeography, Palaeoclimatology, Palaeoecology 392, 510–523.
825 Desmares, D., Grosheny, D., Beaudoin, B., Gardin, S., Gauthier-Lafaye, F., 2007. High resolution
826 stratigraphic record constrained by volcanic ashes layers at the Cenomanian-Turonian boundary
827 in the Western Interior Basin, USA. Cretaceous Research 28, 561–582.
828 Desmares, D., Grosheny, D., Beaudoin, B., 2008. Ontogeny and phylogeny of Upper Cenomanian
829 rotaliporids (Foraminifera). Marine Micropaleontology 69, 91–105.
830 Eicher, D.L., Worstell, P., 1970. Cenomanian and Turonian foraminifera from the Great Plains,
831 United States. Micropaleontology 16, 269–324.
832 Eicher, D.L., 1973. Phylogeny of the late Cenomanian planktonic foraminifer *Anaticinella*
833 *multiloculata* (Morrow). Journal of Foraminiferal Research 2, 184–190.
834 Eicher, D.L., Diner, R., 1985. Foraminifera as indicators of water mass in the Cretaceous Greenhorn
835 Sea, Western Interior. In: Pratt, L.M., Kauffman, E.G., Zelt, F.B. (Eds.), Fine-grained Deposits
836 and Biofacies of the Cretaceous Western Interior Seaway: Evidence of Cyclic Sedimentary
837 Processes, Field Trip Guidebook, Society of Economic Paleontologists and Mineralogists 4, 60–
838 71.
839 Elderbak, K., Leckie, R.M., Tibert, N.E., 2014. Paleoenvironmental and paleoceanographic changes
840 across the Cenomanian–Turonian Boundary Event (Oceanic Anoxic Event 2) as indicated by
841 foraminiferal assemblages from the eastern margin of the Cretaceous Western Interior Sea.
842 Palaeogeography, Palaeoclimatology, Palaeoecology 413, 29–48.

843 Elderbak, K., Leckie, R.M., 2016. Paleocirculation and foraminiferal assemblages of the
844 Cenomanian–Turonian Bridge Creek Limestone bedding couplets: Productivity vs. dilution
845 during OAE2. Cretaceous Research 60, 52–77.
846 Eldrett, J.S., Ma, C., Bergman, S.C., Lutz, B., Gregory, F.J., Dodsworth, P., Phipps, M., Hardas, P.,
847 Minisini, D., Ozkan, A., Ramezani, J., Bowring, S.A., Kamo, S.L., Ferguson, K., Macaulay, C.,
848 Kelly, A.E., 2015. An astronomically calibrated stratigraphy of the Cenomanian, Turonian and
849 earliest Coniacian from the Cretaceous Western Interior Seaway, USA: Implications for global
850 chronostratigraphy. Cretaceous Research 56, 316–344.
851 Erbacher, J., Friedrich, O., Wilson, P.A., Birch, H., Mutterlose, J., 2005. Stable organic carbon
852 isotope stratigraphy across Oceanic Anoxic Event 2 of Demerara Rise, western tropical Atlantic.
853 Geochemistry, Geophysics, Geosystems 6, Q06010, doi:10.1029/2004GC000850.
854 Falzoni, F., Petrizzo, M.R., MacLeod, K.G., Huber, B.T., 2013. Santonian–Campanian planktonic
855 foraminifera from Tanzania, Shatsky Rise and Exmouth Plateau: Species depth ecology and
856 paleoceanographic inferences. Marine Micropaleontology 103, 15–29.
857 Falzoni, F., Petrizzo, M.R., Clarke, L.J., MacLeod, K.G., Jenkyns, H.C., 2016a. Long-term Late
858 Cretaceous oxygen-and carbon-isotope trends and planktonic foraminiferal turnover: A new
859 record from the southern midlatitudes. Geological Society of America Bulletin 128, 1725–1735.
860 Falzoni, F., Petrizzo, M.R., Jenkyns, H.C., Gale, A.S., Tsikos, H., 2016b. Planktonic foraminiferal
861 biostratigraphy and assemblage composition across the Cenomanian–Turonian boundary interval
862 at Clot Chevalier (Vocontian Basin, SE France). Cretaceous Research, 59, 69–97.
863 Forster, A., Schouten, S., Moriya, K., Wilson, P.A., Sinninghe Damsté, J.S., 2007. Tropical
864 warming and intermittent cooling during the Cenomanian/Turonian oceanic anoxic event 2: Sea

surface temperature records from the equatorial Atlantic. Paleoceanography 22, PA1219, doi:10.1029/2006PA001349.

Frush, M.P., Eicher, D.L., 1975. Cenomanian and Turonian foraminifera and paleoenvironments in the Big Bend region of Texas and Mexico. In: Caldwell, W.G.E. (ed.), The Cretaceous System in the Western Interior of North America: The Geological Society of Canada Special Paper 13, p. 277–301.

Gale, A.S., Christensen, W.K., 1996. Occurrence of the belemnite Actinocamax plenus in the Cenomanian of SE France and its significance. Bulletin of the Geological Society of Denmark 43, 68–77.

Gale, A.S., Kennedy, W.J., Voigt, S., Walaszczyk, I., 2005. Stratigraphy of the Upper Cenomanian–Lower Turonian Chalk succession at Eastbourne, Sussex, UK: Ammonites, inoceramid bivalves and stable carbon isotopes. Cretaceous Research 26, 460–487.

Gambacorta, G., Jenkyns, H.C., Russo, F., Tsikos, H., Wilson, P.A., Faucher, G., Erba, E., 2015. Carbon-and oxygen-isotope records of mid-Cretaceous Tethyan pelagic sequences from the Umbria–Marche and Belluno Basins (Italy). Newsletters on Stratigraphy 48, 299–323.

Gebhardt, H., Friedrich, O., Schenk, B., Fox, L., Hart, M.B., and Wagreich, M., 2010. Paleoceanographic changes at the northern Tethyan margin during the Cenomanian–Turonian Oceanic Anoxic Event (OAE-2): Marine Micropaleontology 77, 25–45.

Gonzalez-Donoso, J.M., Linares, D., Robaszynski, F., 2007. The rotaliporids, a polyphyletic group of Albian-Cenomanian planktonic foraminifera: Emendation of genera. Journal of Foraminiferal Research 37, 175–186.

Gradstein, F.M., Ogg, J.G., Schmitz, M.D., Ogg, G.M., 2012. The Geologic Time Scale 2012. Oxford, UK, Elsevier, 1144 p.

888 Grosheny, D., Beaudoin, B., Morel, L., Desmares, D., 2006. High-resolution biostratigraphy and
889 chemostratigraphy of the Cenomanian–Turonian Boundary Event in the Vocontian Basin, S-E
890 France. Cretaceous Research 27, 629–640.
891 Grosheny, D., Ferry, S., Jati, M., Ouaja, M., Bensalah, M., Atrops, F., Chikhi-Aouimeur, F.,
892 Benkerouf-Kechid, F., Negra, H., Salem, H. A., 2013. The Cenomanian–Turonian boundary on
893 the Saharan Platform (Tunisia and Algeria). Cretaceous Research 42, 66–84.
894 Grosheny, D., Ferry, S., Lecuyer, C., Thomas, A., Desmares, D., 2017. The Cenomanian–Turonian
895 Boundary Event (CTBE) on the southern slope of the Subalpine Basin (SE France) and its
896 bearing on a probable tectonic pulse on a larger scale. Cretaceous Research, in press.
897 Hart, M.B., Carter, D.J., 1975. Some observations on the Cretaceous Foraminiferida of southeast
898 England: Journal of Foraminiferal Research 5, 114–126.
899 Hart, M.B., Weaver, P.P.E., 1977. Turonian microbiostratigraphy of Beer, SE Devon: Proceedings
900 of the Ussher Society 4, 86–93.
901 Hart, M.B., Bigg, P.J., 1981. Anoxic events in the Late Cretaceous chalk seas of NW Europe. In:
902 Neale, J. W., Brasier, M. D. (Eds.), Microfossils of Recent and Fossil Shelf Seas: Ellis Horwood
903 Ltd., Chichester, p. 177–185.
904 Hart, M.B., Monteiro, J.F., Watkinson, M.P., Price, G.D., 2002. Correlation of events at the
905 Cenomanian/Turonian boundary: Evidence from Southern England and Colorado. In: Wagreich,
906 M. (Ed.), Aspects of Cretaceous Stratigraphy and Palaeobiogeography. Schriftenreihe der
907 erdwissenschaftliche Kommission der Österreichische Akademie der Wissenschaften, Wien, 15:
908 35–46, Verlag der Österreichische Akademie der Wissenschaften, Wien.
909 Hart, M.B., 2008. Cretaceous foraminifera from the Turonian succession at Beer, southeastern
910 Devon, England. Cretaceous Research 29, 1035–1046.

911 Hasegawa, T., 1999. Planktonic foraminifera and biochronology of the Cenomanian-Turonian
912 (Cretaceous) sequence in the Oyubari area, Hokkaido, Japan. Paleontological Research 3, 173–
913 192.
914 Hay, W.W., DeConto, R., Wold, C.N., Wilson, K.M., Voigt, S., Schulz, M., Wold-Rossby, A.,
915 Dullo, W.C., Ronov, A.B., Balukhovsky, A.N., Soeding, E., 1999. Alternative global Cretaceous
916 paleogeography. In: Barrera, E., Johnson, C.C. (Eds.), The Evolution of the Cretaceous
917 Ocean/climate System. Special Papers of the Geological Society of America 332, 1–47.
918 Haynes, S.J., Huber, B.T., Macleod, K.G., 2015. Evolution and phylogeny of mid-Cretaceous
919 (Albian–Coniacian) biserial planktic foraminifera. Journal of Foraminiferal Research 45, 42–81.
920 Hilbrecht, H., Arthur, M.A., Schlanger, S.O., 1986. The Cenomanian–Turonian boundary event;
921 sedimentary, faunal and geochemical criteria developed from stratigraphic studies in NW
922 Germany. In: Bhattacharji, S., et al. (Eds.), Global Bio- Events; A Critical Approach: Springer,
923 Berlin 8, 345–351.
924 Holbourn, A., Kuhnt, W., 2002. Cenomanian–Turonian palaeoceanographic change on the
925 Kerguelen Plateau: A comparison with Northern Hemisphere records. Cretaceous Research 23,
926 333–349.
927 Huber, B.T., Leckie, R.M., Norris, R.D., Bralower, T.J., CoBabe, E., 1999. Foraminiferal
928 assemblage and stable isotopic change across the Cenomanian-Turonian boundary in the
929 subtropical North Atlantic. Journal of Foraminiferal Research 29, 392–417.
930 Huber, B.T., Petrizzo, M.R., 2014. Evolution and taxonomic study of the Cretaceous planktic
931 foraminiferal genus *Helvetoglobotruncana* Reiss, 1957. Journal of Foraminiferal Research 44,
932 40–57.
933 Ion, J., 1976. A propos de la souche des Rotalipores, *Rotalipora praemontsalvensis* n. sp.: Dări de

Seamă ale Şedinţelor, Institutul de Geologie şi Geofizică Bucharest 62, 39–46.

Jarvis, I., Carson, G.A., Cooper, M.K.E., Hart, M.B., Leary, P.N., Tocher, B.A., Horne, D., Rosenfeld, A., 1988. Microfossil assemblages and the Cenomanian–Turonian (Late Cretaceous) oceanic anoxic event. Cretaceous Research 9, 3–103.

Jarvis, I.A.N., Gale, A.S., Jenkyns, H.C., Pearce, M.A., 2006. Secular variation in Late Cretaceous carbon isotopes: A new $\delta^{13}C$ carbonate reference curve for the Cenomanian–Campanian (99.6–70.6 Ma). Geological Magazine 143, 561–608.

Jarvis, I., Lignum, J.S., Gröcke, D.R., Jenkyns, H.C., Pearce, M.A., 2011. Black shale deposition, atmospheric CO2 drawdown, and cooling during the Cenomanian–Turonian Oceanic Anoxic Event. Paleoceanography 26, PA3201, doi:10.1029/2010PA002081.

Jenkyns, H.C., 2010. Geochemistry of oceanic anoxic events. Geochemistry, Geophysics, Geosystems 11, Q03004, doi:10.1029/2009GC002788.

Jenkyns, H.C., Dickson, A.J., Ruhl, M., Boorn, S.H., 2017. Basalt-seawater interaction, the Plenus Cold Event, enhanced weathering and geochemical change: Deconstructing Oceanic Anoxic Event 2 (Cenomanian–Turonian, Late Cretaceous). Sedimentology 64, 16–43.

Keller, G., Han, Q., Adatte, T., Burns, S., 2001. Paleoenvironment of the Cenomanian-Turonian transition at Eastbourne, England. Cretaceous Research 22, 391–422.

Keller, G., Pardo, A., 2004. Age and paleoenvironment of the Cenomanian-Turonian global stratotype section and point at Pueblo, Colorado. Marine Micropaleontology 51, 95–128.

Keller, G., Berner, Z., Adatte, T., Stueben, D., 2004. Cenomanian–Turonian and $\delta^{13}C$, and $\delta^{18}O$, sea level and salinity variations at Pueblo, Colorado. Palaeogeography, Palaeoclimatology, Palaeoecology 211, 19–43.

Keller, G., Adatte, T., Berner, Z., Chellai, E.H., Stueben, D., 2008. Oceanic events and biotic effects of the Cenomanian-Turonian anoxic event, Tarfaya Basin, Morocco. Cretaceous Research 29, 976–994.

Kennedy, W.J., Cobban, W.A., Elder, W.P., Kirkland, J.I., 1999. Lower Turonian (Upper Cretaceous) *Watinoceras devonense* Zone ammonite fauna in Colorado, USA. Cretaceous Research 20, 629–639.

Kennedy, W.J., Walaszczyk, I., Cobban, W.A., 2000. Pueblo, Colorado, USA, Candidate Global Boundary Stratotype Section and Point for the base of the Turonian Stage of the Cretaceous and for the Middle Turonian substage, with a revision of the Inoceramidae (Bivalvia). Acta Geologica Polonica 50, 295–334.

Kennedy, W.J., Walaszczyk, I., Cobban, W.P., 2005. The Global Boundary Stratotype Section and Point for the base of the Turonian Stage of the Cretaceous: Pueblo, Colorado, USA. Episodes 28, 93–104.

Kopaevich, L., Vishnevskaya, V., 2016. Cenomanian–Campanian (Late Cretaceous) planktonic assemblages of the Crimea–Caucasus area: Palaeoceanography, palaeoclimate and sea level changes. Palaeogeography, Palaeoclimatology, Palaeoecology 441, 493–515.

Kuhnt, W., Nederbragt, A., Leine, L., 1997. Cyclicity of Cenomanian – Turonian organic-carbon-rich sediments in the Tarfaya Atlantic Coastal Basin (Morocco). Cretaceous Research 18, 587–601.

Kuhnt, W., Luderer, F., Nederbragt, S., Thurow, J., Wagner, T., 2005. Orbital-scale record of the late Cenomanian–Turonian oceanic anoxic event (OAE-2) in the Tarfaya Basin (Morocco). International Journal of Earth Sciences 94, 147–159.

978 Lamolda, M.A., Gorostidi, A., Martínez, R., López, G., Peryt, D., 1997. Fossil occurrences in the
979 Upper Cenomanian–Lower Turonian at Ganuza, northern Spain: An approach to
980 Cenomanian/Turonian boundary chronostratigraphy. Cretaceous Research 18, 331–353.
981 Leckie, R.M., 1985. Foraminifera of the Cenomanian–Turonian boundary interval, Greenhorn
982 Formation, Rock Canyon Anticline, Pueblo, Colorado. In: Pratt, L.M., Kauffman, E.G., Zelt,
983 F.B. (Eds.), Fine-grained Deposits and Biofacies of the Cretaceous Western Interior Seaway:
984 Evidence of Cyclic Sedimentary Processes, Field Trip Guidebook, Society of Economic
985 Paleontologists and Mineralogists 4, 139–149.
986 Leckie, R.M., Yuretrich, R.F., West, O.L.O., Finkelstein, D., Schmidt, M., 1998. Paleoceanography
987 of the southwestern Western Interior Sea during the time of the Cenomanian–Turonian boundary
988 (Late Cretaceous). In: Dean, W., Arthur, M.A. (Eds.), Stratigraphy and Paleoenvironments of the
989 Cretaceous Western Interior Seaway. SEPM Concepts in Sedimentology and Paleontology 6,
990 101–126.
991 Leckie, R.M., Bralower, T.J., Cashman, R., 2002. Oceanic anoxic events and plankton evolution:
992 Biotic response to tectonic forcing during the mid-Cretaceous. Paleoceanography 17, doi:
993 10.1029/2001PA000623.
994 Lipson-Benitah, S., Rosenfeld, A., Akira Flexer, A.H., Kashai, E., 1988. The middle Turonian
995 Daliyya type section in Israel: Biostratigraphy, palaeoenvironment and sea-level changes.
996 Cretaceous Research 9, 321–336.
997 Lirer, F., 2000. A new technique for retrieving calcareous microfossils from lithified lime deposits.
998 Micropaleontology 46, 365–369.
999 Longoria, J.F., 1973. *Pseudoticinella*, a new genus of planktonic foraminifera from the early
1000 Turonian of Texas. Revista Española de Micropaleontología 5, 417–423.

1001 Lowery, C.M., Corbett, M.J., Leckie, R.M., Watkins, D., Miceli Romero, A., Pramudito, A., 2014.
1002 Foraminiferal and nannofossil paleoecology and paleoceanography of the Cenomanian–Turonian
1003 Eagle Ford Shale of southern Texas. Palaeogeography, Palaeoclimatology, Palaeoecology 413,
1004 49–65.
1005 Lowery, C.M., Leckie, R.M., 2017. Biostratigraphy of the Cenomanian-Turonian Eagle Ford Shale
1006 of South Texas. Journal of Foraminiferal Research 47, 105–128.
1007 Luciani, V., Cobianchi, M., 1999. The Bonarelli Level and other black shales in the Cenomanian-
1008 Turonian of the northeastern Dolomites (Italy): calcareous nannofossil and foraminiferal data.
1009 Cretaceous Research 20, 135–167.
1010 Meyers, S.R., Sageman, B.B., and Hinnov, L.A., 2001. Integrated quantitative stratigraphy of the
1011 Cenomanian-Turonian Bridge Creek Limestone Member using evolutive harmonic analysis and
1012 stratigraphic modeling. Journal of Sedimentary Research 71, 628–644.
1013 Meyers, S.R., Siewert, S.E., Singer, B.S., Sageman, B.B., Condon, D.J., Obradovich, J.D., Jicha,
1014 B.R., Sawyer, D.A., 2012. Intercalibration of radioisotopic and astrochronologic time scales for
1015 the Cenomanian-Turonian boundary interval, Western Interior Basin, USA. Geology 40, 7–10.
1016 Morrow, A.L., 1934. Foraminifera and Ostracoda from the Upper Cretaceous of Kansas. J.
1017 Paleontol. 8, 186–205.
1018 Mort, H., Jacquat, O., Adatte, T., Steinmann, P., Föllmi, K., Matera, V., Berner, Z., Stüben, D.,
1019 2007. The Cenomanian/Turonian anoxic event at the Bonarelli Level in Italy and Spain:
1020 Enhanced productivity and/or better preservation? Cretaceous Research 28, 597–612.
1021 Nederbragt, A.J., Fiorentino, A., 1999. Stratigraphy and palaeoceanography of the Cenomanian–
1022 Turonian Boundary Event in Oued Mellegue, north-western Tunisia. Cretaceous Research 20,
1023 47–62.

1024 Pagani, M., Arthur, M.A., 1998. Stable isotopic studies of the Cenomanian–Turonian proximal
1025 marine fauna from the U.S. Western Interior Seaway. In: Dean, W.E., Arthur, M.A. (Eds.),
1026 SEPM Concepts in Sedimentology and Paleontology, vol. 6. SEPM, Tulsa, USA, pp. 201–225.
1027 Paul, C.R.C., Lamolda, M.A., Mitchell, S.F., Vaziri, M.R., Gorostidi, A., Marshall, J.D., 1999. The
1028 Cenomanian–Turonian boundary at Eastbourne (Sussex, UK): A proposed European reference
1029 section. Palaeogeography, Palaeoclimatology, Palaeoecology 150, 83–121.
1030 Paul, C.R.C., Lamolda, M.A., 2009. Testing the precision of bioevents. Geological Magazine 146,
1031 625–637.
1032 Pearce, M.A., Jarvis, I., Tocher, B.A., 2009. The Cenomanian–Turonian boundary event, OAE2 and
1033 palaeoenvironmental change in epicontinental seas: New insights from the dinocyst and
1034 geochemical records. Palaeogeography, Palaeoclimatology, Palaeoecology 280, 207–234.
1035 Pessagno, E.A., Jr., 1967. Upper Cretaceous planktonic foraminifera from the western Gulf Coastal
1036 Plain. Paleontographica Americana 5, 245–445.
1037 Petrizzo, M.R., 2000. Upper Turonian–lower Campanian planktonic foraminifera from southern
1038 mid–high latitudes (Exmouth Plateau, NW Australia): biostratigraphy and taxonomic notes.
1039 Cretaceous Research 21, 479–505.
1040 Petrizzo, M.R., 2001. Late Cretaceous planktonic foraminifera from Kerguelen Plateau (ODP Leg
1041 183): New data to improve the Southern Ocean biozonation: Cretaceous Research 22, 829–855.
1042 Petrizzo, M.R., Falzoni, F., Premoli Silva, I., 2011. Identification of the base of the lower-to-middle
1043 Campanian *Globotruncana ventricosa* Zone: Comments on reliability and global correlations.
1044 Cretaceous Research 32, 387–405.
1045 Petrizzo, M.R., Jiménez Berrocoso, Á., Falzoni, F., Huber, B.T., MacLeod, K.G., 2017. The
1046 Coniacian–Santonian sedimentary record in southern Tanzania (Ruvuma Basin, East Africa):

1047 Planktonic foraminiferal evolutionary, geochemical and palaeoceanographic patterns.
1048 Sedimentology 64, 252–285.
1049 Pratt, L.M., 1984. Influence of paleoenvironmental factors on preservation of organic matter in
1050 Middle Cretaceous Greenhorn Formation, Pueblo, Colorado. AAPG Bulletin 68, 1146–1159.
1051 Pratt, L.M., Threlkeld, C.N., 1984. Stratigraphic significance of $^{13}C/^{12}C$ ratios in mid-Cretaceous
1052 rocks of the Western Interior. Memoir of the Canadian Society of Petroleum Geologists 9, 305–
1053 312.
1054 Pratt, L.M., 1985. Isotopic studies of organic matter and carbonate in rocks of the Greenhorn
1055 marine cycle. In: Pratt, L.M., Kauffman, E.G., Zelt, F.B. (Eds.), Fine-grained Deposits and
1056 Biofacies of the Cretaceous Western Interior Seaway: Evidence of Cyclic Sedimentary
1057 Processes, Field Trip Guidebook, Society of Economic Paleontologists and Mineralogists 4, 38–
1058 48.
1059 Pratt, L.M., Arthur, M.A., Dean, W.E., Scholle, P.A. 1993. Paleo-oceanographic cycles and events
1060 during the Late Cretaceous in the Western Interior Seaway of North America. In: Caldwell,
1061 W.G.E., Kauffman, E.G. (Eds.), Geological Association of Canada Special Paper 39, 333–353.
1062 Premoli Silva, I., Sliter, W.V., 1995. Cretaceous planktonic foraminiferal biostratigraphy and
1063 evolutionary trends from the Bottaccione section, Gubbio, Italy. Palaeontographia Italica 81, 2–
1064 90.
1065 Premoli Silva, I., Sliter, W.V., 1999. Cretaceous paleoceanography: Evidence from planktonic
1066 foraminiferal evolution. In: Barrera, E., Johnson, C.C., (Eds.), The Evolution of the Cretaceous
1067 Ocean-Climate System. Special Papers of the Geological Society of America 332, 301–328,
1068 doi:10.1130/0-8137-2332-9.301.

1069 Premoli Silva, I., Erba, E., Salvini, G., Locatelli, C., Verga, D., 1999. Biotic changes in Cretaceous
1070 oceanic anoxic events of the Tethys. Journal of Foraminiferal Research 29, 352–370.
1071 Robaszynski, F., Caron, M., le Groupe de Travail Européen des Foraminifères Planctoniques, 1979.
1072 Atlas des Foraminifères Planctoniques du Crétacé Moyen (Mer Boréale et Téthys). Cahiers de
1073 Micropaléontologie 1, 1–185; 2, 1–181.
1074 Robaszynski, F., Caron, M., Dupuis, C., Amédro, F., Gonzalez-Donoso, J.M., Linares, D.,
1075 Hardenbol, J., Gartner, S., Calandra, F., Deloffre, R., 1990. A tentative integrated stratigraphy in
1076 the Turonian of Central Tunisia: formations, zones and sequential stratigraphy in the Kalaat
1077 Senan area. Bulletin des Centres de Recherches Exploration-Production Elf Aquitaine 14, 213–
1078 384.
1079 Robaszynski, F., Caron, M., Amédro, F., Dupuis, C., Hardenbol, J., Gonzalez-Donoso, J.M.,
1080 Linares, D., Gartner, S., 1993. Le Cénomanien de la region de Kalaat Senan (Tunisie Centrale):
1081 litho-biostratigraphie et interpretation séquentielle. Revue de Paléobiologie 12, 351–505.
1082 Robaszynski, F., Caron, M., 1995. Foraminiféres planctoniques du Crétacé: commentaire de la
1083 zonation Europe-Méditerranée. Bulletin de la Société Géologique de France 166, 681–692.
1084 Robaszynski, F., Gale, A., Juignet, P., Amédro, F., & Hardenbol, J., 1998. Sequence stratigraphy in
1085 the Upper Cretaceous series of the Anglo-Paris Basin: exemplified by the Cenomanian stage. In:
1086 de Graciansky, P.-C., et al. (Eds.), Mesozoic and Cenozoic sequence stratigraphy of European
1087 Basins. SEPM Special Publications 60, 363–386.
1088 Sadler, P.M., 2004. Quantitative biostratigraphy-Achieving finer resolution in global correlation.
1089 Annual Review Earth and Planetary Sciences 32, 187–213.
1090 Sageman, B.B., Meyers, S.R., Arthur, M.A., 2006. Orbital time scale and new C-isotope record for
1091 Cenomanian-Turonian boundary stratotype. Geology 34, 125–128.

1092 Schlanger, S.O., Jenkyns, H.C., 1976. Cretaceous oceanic anoxic events: Causes and consequences.
1093 Geologie en Mijnbouw 55, 179–184.
1094 Schlanger, S.O., Arthur, M.A., Jenkyns, H.C., Scholle, P.A., 1987. The Cenomanian-Turonian
1095 Oceanic Anoxic Event, I. Stratigraphy and distribution of organic carbon-rich beds and the
1096 marine δ13C excursion. Geological Society, London, Special Publications 26, 371–399.
1097 Scholle, P.A., Arthur, M.A., 1980. Carbon isotope fluctuations in Cretaceous pelagic limestones:
1098 Potential stratigraphic and petroleum exploration tool. American Association of Petroleum
1099 Geologists Bulletin 64, 67–87.
1100 Scopelliti, G., Bellanca, A., Coccioni, R., Luciani, V., Neri, R., Baudin, F., Chiari, M., Marcucci,
1101 M., 2004. High-resolution geochemical and biotic records of the Tethyan "Bonarelli Level"
1102 (OAE2, latest Cenomanian) from the Calabianca–Guidaloca composite section, northwestern
1103 Sicily, Italy. Palaeogeography, Palaeoclimatology, Palaeoecology 208, 293–317.
1104 Shaw, A.B., 1964. Time in stratigraphy. McGraw-Hill, New York, USA, 365 pp.
1105 Sinninghe Damsté, J.S., van Bentum, E.C., Reichart, G.J., Pross, J., Schouten, S., 2010. A CO_2
1106 decrease-driven cooling and increased latitudinal temperature gradient during the mid-
1107 Cretaceous Oceanic Anoxic Event 2. Earth and Planetary Science Letters 293, 97–103.
1108 Sliter, W.V., 1989. Biostratigraphic zonation for Cretaceous planktonic foraminifers examined in
1109 thin section. The Journal of Foraminiferal Research 19, 1–19.
1110 Tsikos, H., Jenkyns, H.C., Walsworth-Bell, B., Petrizzo, M.R., Forster, A., Kolonic, S., Erba, E.,
1111 Premoli Silva, I., Baas, M., Wagner, T., Sinninghe Damsté, J.S., 2004. Carbon-isotope
1112 stratigraphy recorded by the Cenomanian–Turonian Oceanic Anoxic Event: Correlation and
1113 implications based on three localities. Journal of the Geological Society of London 161, 711–
1114 719.

1115 Tur, N. A., Smirnov, J. P., Huber, B. T., 2001. Late Albian–Coniacian planktic foraminifera and
1116 biostratigraphy of the northeastern Caucasus: Cretaceous Research 22, 719–734.
1117 Voigt, S., Aurag, A., Leis, F., Kaplan, U., 2007. Late Cenomanian to Middle Turonian high-
1118 resolution carbon isotope stratigraphy: New data from the Münsterland Cretaceous Basin,
1119 Germany. Earth and Planetary Science Letters 253, 196–210.
1120 Voigt, S., Erbacher, J., Mutterlose, J., Weiss, W., Westerhold, T., Wiese, F., Wilmsen, M., Wonik,
1121 T., 2008. The Cenomanian – Turonian of the Wunstorf section – (North Germany): Global
1122 stratigraphic reference section and new orbital time scale for Oceanic Anoxic Event 2.
1123 Newsletters on Stratigraphy 43, 65–89.
1124 West, O.L., Leckie, R.M., Schmidt, M., 1998. Foraminiferal paleoecology and paleoceanography of
1125 the Greenhorn cycle along the southwestern margin of the Western Interior Sea. SEPM,
1126 Concepts in Sedimentology and Paleontology 6, 79–99.
1127 Westermann, S., Caron, M., Fiet, N., Fleitmann, D., Matera, V., Adatte, T., Föllmi, K.B., 2010.
1128 Evidence for oxic conditions during oceanic anoxic event 2 in the northern Tethyan pelagic
1129 realm. Cretaceous Research 31, 500–514.
1130 Wonders, A.A.H., 1980. Middle and Late Cretaceous planktonic foraminifera of the western
1131 Mediterranean area. Utrecht Micropaleontological Bulletin 24, 1–157.
1132
1133
1134 **Taxonomic Appendix**
1135 List of planktonic foraminiferal species with authors and years mentioned in the text and/or in the
1136 figures.
1137

Dicarinella canaliculata (Reuss, 1854)

Dicarinella elata Lamolda, 1977

Dicarinella hagni (Scheibnerova, 1962)

Dicarinella imbricata (Mornod, 1950)

Falsotruncana maslakovae Caron, 1981

"Globigerinelloides" bentonensis (Morrow, 1934). The genus *Globigerinelloides* is herein indicated in brackets, as it is currently under revision by the Mesozoic Planktonic Foraminiferal Working Group see Taxonomic notes in Petrizzo et al. (2017).

Helvetoglobotruncana helvetica (Bolli, 1945)

Helvetoglobotruncana praehelvetica (Trujillo, 1960)

Marginotruncana coronata (Bolli, 1945)

Marginotruncana marianosi (Douglas, 1969)

Marginotruncana renzi (Gandolfi, 1942)

Marginotruncana schneegansi (Sigal, 1952)

Marginotruncana sigali (Reichel, 1950)

Planoheterohelix moremani (Cushman, 1938)

Planoheterohelix paraglobulosa (Georgescu and Huber, 2009)

Praeglobotruncana algeriana Caron, 1966

Praeglobotruncana oraviensis Scheibnerova, 1960

Rotalipora cushmani (Morrow, 1934)

Rotalipora montsalvensis (Mornod, 1950)

Rotalipora praemontsalvensis Ion, 1976

Rotalipora planoconvexa (Longoria, 1973)

Thalmanninella brotzeni Sigal, 1948

Thalmanninella deeckei (Franke, 1925)

Thalmanninella globotruncanoides (Sigal, 1948)

Thalmanninella greenhornensis (Morrow, 1934)

Thalmanninella multiloculata (Morrow, 1934)

Whiteinella aprica (Loeblich and Tappan, 1961)

Whiteinella archaeocretacea Pessagno, 1967

Figure captions

TABLE 1. Source of planktonic foraminiferal bioevents and biostratigraphy, methodology used to process samples, $\delta^{13}C_{carb}$ and $\delta^{13}C_{org}$ profiles available in the literature for each section treated in this study.

TABLE 2. Mean depth and age of the events constrained by the age-depth model for the Pueblo section. Age of bentonites and of the C/T boundary (LO of *W. devonense*) are from Meyers et al. (2012). The ages of the other bioevents are calculated in this study.

TABLE 3. Depth and source of bio- and chemostratigraphic events identified at Pueblo, Eastbourne and Tarfaya that were used to perform the graphic correlations illustrated in Fig. 7.

FIGURE 1. Paleogeographic reconstruction for the late Cenomanian (94 Ma), with location of sections examined during this study (after Hay et al., 1999).

1184

1185 FIGURE 2. Pueblo, Colorado (Western Interior Seaway). The C/T boundary is placed between the
1186 top of the *N. juddii* and the base of the *W. devonense* Zone according to Caron et al. (2006).
1187 Lithostratigraphy is from Kennedy et al. (2005) and stratigraphic logs with position of bentonites
1188 are from Kennedy et al. (2005) and Caron et al. (2006). Bed numbers are according to Cobban and
1189 Scott (1972). Ammonite biostratigraphy is after Kennedy et al. (1999, 2000). $\delta^{13}C_{carb}$ profile and
1190 position of peak I, II and III are after Caron et al. (2006). The $\delta^{13}C_{org}$ profile of the nearby PU-79
1191 core (Pratt and Threlkeld, 1984; Pratt, 1985) is correlated with the Rock Canyon outcrop using
1192 marker beds. Planktonic foraminiferal bioevents are after Eicher and Diner (1985), Leckie (1985),
1193 Leckie et al. (1998), Keller and Pardo (2004), Caron et al. (2006), Desmares et al. (2007) and
1194 Elderbak and Leckie (2016). The top of the *R. cushmani* Zone is placed according to Leckie (1985),
1195 while the base of the *H. helvetica* Zone is according to Elderbak and Leckie (2016), see text for
1196 further explanations. Calcareous nannofossil events are after Tsikos et al. (2004).

1197

1198 FIGURE 3. Eastbourne (UK). On the left: lithostratigraphy, planktonic foraminiferal
1199 biostratigraphy and $\delta^{13}C_{carb}$ profile (black) after Tsikos et al. (2004), age/stage and ammonite
1200 biostratigraphy after Gale et al. (2005). On the right: age/stage, lithostratigraphy, planktonic
1201 foraminiferal and ammonite biostratigraphy after Paul et al. (1999). The $\delta^{13}C_{carb}$ profile (grey) is
1202 according to Paul et al. (1999) and refers to the stratigraphic log on the right. Chemostratigraphic
1203 peaks (A, B, C) are after Jarvis et al. (2006) and Voigt et al. (2008) (see text for further details). The
1204 samples examined in this study refer to the stratigraphic log by Tsikos et al. (2004) in the left.
1205 Erosional basal surfaces are according to Keller et al. (2001). Planktonic foraminiferal events after

1206 Paul et al. (1999), Keller et al. (2001), Hart et al. (2002), Tsikos et al. (2004) and this study.
1207 Calcareous nannofossil events are according to Tsikos et al. (2004).
1208
1209 FIGURE 4. Planktonic foraminiferal specimens from the Eastbourne section. (1a–c) *Rotalipora*
1210 *cushmani*, sample GC-600 (0 m, base of the section). (2a–c) *Praeglobotruncana algeriana*, sample
1211 GC-260 (3.4 m). (3a–c) *Dicarinella hagni*, sample WC1240 (26.3 m). (4a–c) *Dicarinella imbricata*,
1212 sample GC-480 (1.2 m). (5a–c) *Helvetoglobotruncana praehelvetica*, sample GC-360 (2.4 m). (6a–
1213 c) *Dicarinella elata*, sample WC360 (17.5 m). (7a–c) *Thalmanninella brotzeni*, sample GC-340 (2.6
1214 m). (8a–c) *Thalmanninella greenhornensis*, sample GC-260 (3.4 m). (9a–c) *Thalmanninella*
1215 *deeckei*, sample GC-260 (3.4 m). (10a–c) *Praeglobotruncana oraviensis*, sample PM+280 (8.8 m).
1216 Scale bar = 100 μm.
1217
1218 FIGURE 5. Planktonic foraminiferal specimens from Eastbourne and Tarfaya. Eastbourne: (1a–c)
1219 *Rotalipora montsalvensis*, sample GC-500 (1 m). (2a–c) *Rotalipora praemontsalvensis*, sample
1220 PM+240 (8.4 m). (3a–c) *Whiteinella archaeocretacea*, sample GC-540 (0.6 m). Tarfaya: (4a–c)
1221 *Helvetoglobotruncana praehelvetica*, sample S57/T58, 45–51 cm (depth 57.25 m). (5a–c)
1222 *Thalmanninella deeckei*, sample S57/T57, 61–66 cm (depth 56.50 m). (6a–c) *Thalmanninella*
1223 *greenhornensis*, sample S57/T67, 9–14 cm (depth 59.55 m). (7a–c) "*Globigerinelloides"*
1224 *bentonensis*, sample S57/T59, 38–43 cm (depth 58.16 m). (8a–b) *Planoheterohelix moremani*,
1225 sample S57/T58, 45–51 cm (depth 57.25 m). (9a–b) *Planoheterohelix paraglobulosa*, sample
1226 S57/T58, 45–51 cm (depth 57.25 m). (10a–c) *Praeglobotruncana algeriana*, sample S57/T57, 61–
1227 66 cm (depth 56.50 m). (11a–c) *Dicarinella hagni*, sample S57/T57, 61–66 cm (depth 56.50 m).
1228 Scale bar = 100 μm.

1229

1230 FIGURE 6. Tarfaya, core S57 (Morocco): planktonic foraminiferal biozonation, calcareous
1231 nannofossil events, position of the C/T boundary and $\delta^{13}C_{org}$ profile after Tsikos et al. (2004) and
1232 Jenkyns et al. (2017). Planktonic foraminiferal and chemostratigraphic events according to this
1233 study.

1234

1235 FIGURE 7. Age-depth model for the Pueblo section. The age model is constrained by bentonite
1236 ages as calculated by Meyers et al. (2012). The linear functions obtained are as follows: 1)
1237 Bentonite A to Bentonite B (y=-9.5x+897.16); 2) Bentonite B to LO of *W. devonense* (y=-
1238 8.2353x+778.19); 3) LO of *W. devonense* to Bentonite C (y=-6.3636x+602.45); 4) Bentonite C to
1239 Bentonite D (y=-6.8462x+647.7).

1240

1241 FIGURE 8. Graphic correlations: 8a) Depth-depth plot of Pueblo vs. Eastbourne and 8b) depth-
1242 depth plot of Pueblo vs. Tarfaya. Please note that the depth of the LO of *Q. gartneri* at Tarfaya is
1243 represented with the error bar because its precise position is uncertain and likely falls within the
1244 coring gap (Tsikos et al., 2004).

1245

1246 FIGURE 9. Planktonic foraminiferal bioevents identified in each section plotted against a simplified
1247 $\delta^{13}C$ profile. The methodology applied to study planktonic foraminifera (washed residues and/or
1248 thin sections) is indicated for each locality. Reliable bioevents are in green, potentially useful
1249 bioevents are in blue. Misleading bioevents include (1) ecologically controlled bioevents (purple),
1250 (2) unreliable bioevents because of taxonomic uncertainties, subjective species concepts and
1251 transitional evolution from ancestor species (red), and (3) possibly delayed appearances because of

species rare occurrence, low sampling resolution and/or small sample size (orange). Misleading bioevents are categorized according to the most important factor that in our opinion controlled species diachronism, in case multiple options are possible. The HO of *R. cushmani* at Clot Chevalier is in black, because its position is controlled by the sedimentologic features of the section. See text for references and discussion.

FIGURE 10. Summary of the most reliable sequence of planktonic foraminiferal bioevents for mid-low latitudes correlation across the C–T boundary interval and list of the bioevents that appear potentially useful but require further calibration in other localities. Reliable bioevents are numbered in stratigraphic order from the bottom to the top.

FIGURE 11. SEM images of the washed residues obtained from the rock samples collected at Eastbourne showing the composition of the assemblage in the <125 μm size-fraction with dominant calcispheres and rare biserial taxa. 1) Sample WC300 (16.9 m); 2) sample WC500 (18.9 m); 3) sample WC800 (21.9 m); and 4) sample WC1300 (26.9 m). Scale bar = 200 μm.

Supplementary materials

FIGURE A. Clot Chevalier section (Vocontian Basin, SE France): age/stage, lithostratigraphy, planktonic foraminiferal biostratigraphy and bioevents, $\delta^{13}C_{carb}$ profile and chemostratigraphic events after Falzoni et al. (2016b).

FIGURE B. Pont d'Issole section (Vocontian Basin, SE France): the chemostratigraphic events are after Jarvis et al. (2006), with the exception of peak C (grey in the figure) that is herein placed based on the definition given in the text. The position of the C/T boundary is here estimated to fall within the interval from the estimated LO of *W. devonense* based on the bio- and chemostratigraphic correlation with Eastbourne (see Jarvis et al., 2011) and the LO of *H. helvetica* and includes peak C (as positioned in this study). Lithostratigraphy is according to Jarvis et al. (2006). Planktonic foraminiferal biostratigraphy and bioevents are from Grosheny et al. (2006). The $\delta^{13}C_{carb}$ profiles are from Grosheny et al. (2006) and Jarvis et al. (2006).

FIGURE C. Wadi Bahloul section (Tunisia): age/stage, lithostratigraphy, ammonite zonation, planktonic foraminiferal biostratigraphy and bioevents, $\delta^{13}C_{carb}$ profile and chemostratigraphic events (I, II, and III) from Caron et al. (2006). A, B, and C peaks are here placed according to the definition provided in this study.

FIGURE D. Gongzha section (Tibet): formations, planktonic foraminiferal biostratigraphy and bioevents, $\delta^{13}C_{carb}$ profile and chemostratigraphic events from Bomou et al. (2013). The position of the C/T boundary is here estimated to fall within the interval from peak C and the LO of *H. helvetica*.

Sections	Planktonic foraminiferal bioevents and biostratigraphy	Methods for planktonic foraminiferal study	available $\delta^{13}C_{carb}$ data (bulk)	available $\delta^{13}C_{org}$ data (bulk)
Eastbourne	Paul et al., 1999 Keller et al., 2001 Hart et al., 2002 Tsikos et al., 2004 this study	washed residues washed residues not specified washed residues + thin sections washed residues	Paul et al., 1999 Tsikos et al., 2004	Paul et al., 1999 Keller et al., 2001 Tsikos et al., 2004
Tarfaya, core S57	Tsikos et al., 2004 this study	washed residues washed residues	Tsikos et al., 2004	Tsikos et al., 2004
Pueblo	Eicher and Worstell, 1970 Eicher and Diner, 1985 Leckie, 1985 Leckie et al., 1998 West et al., 1998 Keller and Pardo, 2004 Caron et al., 2006 Desmares et al., 2007 Elderbak and Leckie	washed residues washed residues washed residues washed residues washed residues washed residues washed residues + thin sections washed residues + thin sections washed residues	*Rock Canyon*: Caron et al., 2006; *PU-79 Core*: Pratt 1985; Pratt et al.1993 *Portland Core*: Sageman et al., 2006	*Rock Canyon:* Bowman and Bralower, 2005; *PU-79 Core*: Pratt and Threlkeld, 1984; Pratt 1985; Pratt et al. 1993 *Portland Core*: Sageman et al., 2006
Clot Chevalier	Falzoni et al., 2016b	washed residues	Falzoni et al., 2016b	
Pont d'Issole	Grosheny et al., 2006	washed residues + thin sections	Grosheny et al., 2006 Jarvis et al., 2011	Jarvis et al., 2011
wadi Bahloul	Caron et al., 2006	washed residues + thin sections	Caron et al., 2006	
Gongzha	Bomou et al., 2013	thin sections	Bomou et al., 2013	

Table 1

ROCK CANYON, PUEBLO (COLORADO)

Events	mean depth (m)	Age (Ma)
LO *H. helvetica*	7.75	93.48
LO *M. marianosi*	7.70	93.48
Bentonite D	**6.49**	**93.66**
Bentonite C	**5.60**	**93.79**
LO *W. devonense* - C/T boundary	**4.90**	**93.90**
Bentonite B	**3.50**	**94.07**
"*Heterohelix* shift"	2.80	94.14
Bentonite A	**1.60**	**94.27**
HO *"G". bentonensis*	1.55	94.28
HO *Th. greenhornensis*	1.45	94.29
HO *R. cushmani*	1.45	94.29
LO *H. prahelvetica*	0.45	94.39
HO *Th. deeckei*	0.40	94.39
LO *D. canaliculata*	-0.75	94.51
LO *D. elata*	-0.75	94.51
LO *D. imbricata*	-0.75	94.51
LO *D. hagni*	-1.20	94.55
LO *P. algeriana*	-1.20	94.55

Table 2

Pueblo

Events	mean depth (m)	Source
LO *D. canaliculata*	-0.75	Caron et al. (2006)
LO *D. elata*	-0.75	Caron et al. (2006)
HO *Th. deeckei*	0.40	Eicher and Diner (1985)
LO *H. praehelvetica*	0.45	Caron et al. (2006)
δ^{13}C peak A	1.30	Pratt and Threlkeld (1984)
HO *Th. greenhornensis*	1.45	Leckie (1985)
HO *R. cushmani*	1.45	Leckie (1985)
HO "*G." bentonensis*	1.55	Leckie (1985)
HO *A. albianus*	1.90	Tsikos et al. (2004)
δ^{13}C peak B	2.60	Pratt and Threlkeld (1984)
onset *"Heterohelix* shift"	2.80	Leckie et al. (1998)
LO *N. juddii*	2.95	Caron et al. (2006)
δ^{13}C peak C	4.65	Pratt and Threlkeld (1984)
LO *W. devonense*	4.90	Caron et al. (2006)
LO *Q. gartneri*	5.85	Tsikos et al. (2004)

Eastbourne

Events	mean depth (m)	Source
LO *D. canaliculata*	3.00	this study
LO *D. elata*	3.80	this study
HO *Th. deeckei*	8.30	this study
LO *H. praehelvetica*	2.20	this study
δ^{13}C peak A	10.40	Jarvis et al. (2006)
HO *Th. greenhornensis*	8.30	this study
HO *R. cushmani*	11.30	Tsikos et al. (2004)
HO "*G." bentonensis*	13.10	this study
HO *A. albianus*	12.80	Tsikos et al. (2004)
δ^{13}C peak B	14.10	Jarvis et al. (2006)
LO *N. juddii*	14.85	Gale et al. (2005)
δ^{13}C peak C	17.90	Voigt et al. (2008)
base *W. devonense* Zone	17.90	Gale et al. (2005)
LO *Q. gartneri*	18.60	Tsikos et al. (2004)
δ^{13}C peak C	19.70	Jarvis et al. (2006)

Tarfaya

Events	mean depth (m)	Source
HO *Th. deeckei*	54.06	this study
LO *H. praehelvetica*	55.015	this study
δ^{13}C peak A	52.920	this study
HO *Th. greenhornensis*	53.845	this study
HO *R. cushmani*	50.86	Tsikos et al. (2004)
HO "*G." bentonensis*	50.085	this study
HO *A. albianus*	53.845	Tsikos et al. (2004)
δ^{13}C peak B	51.13	this study
onset *"Heterohelix* shift"	50.255	this study
δ^{13}C peak C	44.61	this study
LO *Q. gartneri*	43.320	Tsikos et al. (2004)

Table 3

Fig. 1

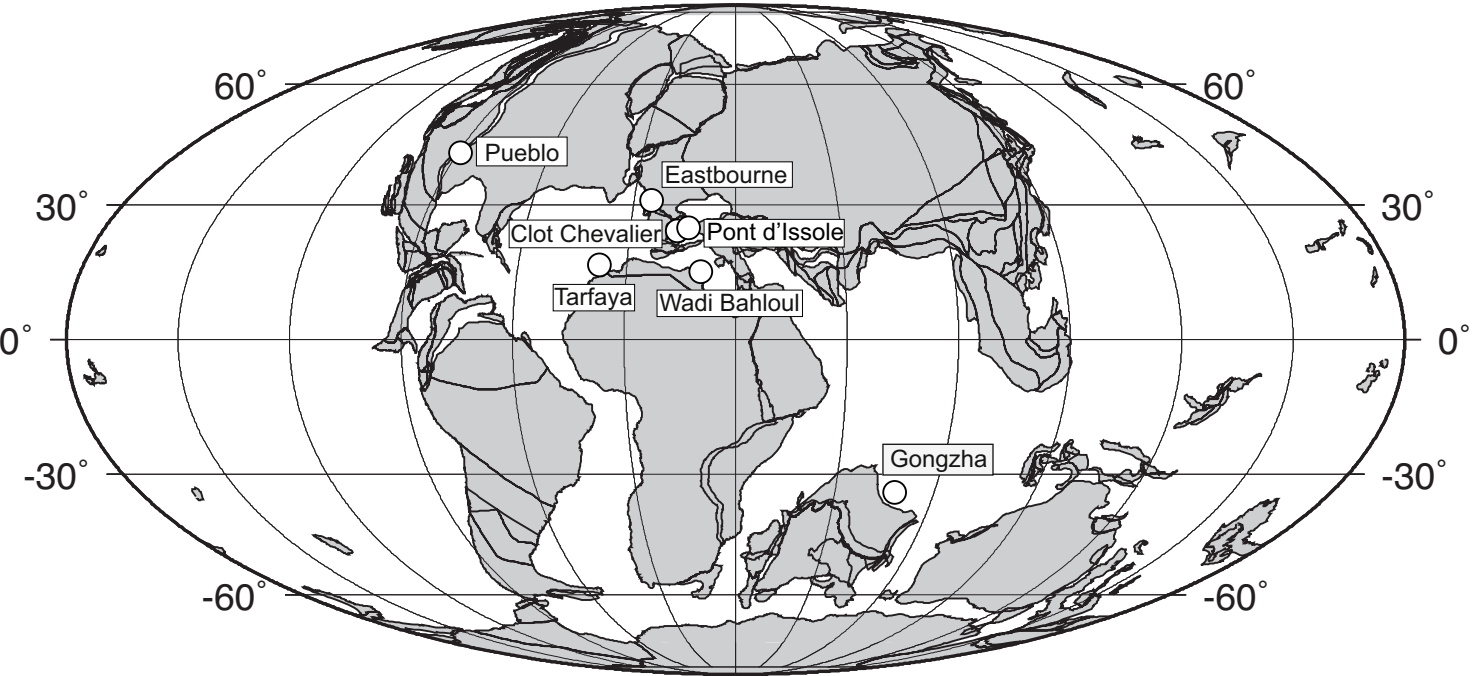
60˚
60˚
30˚
30˚
0˚
0˚
-30˚
-30˚
-60˚
-60˚
Pueblo
Eastbourne
Clot Chevalier
Pont d'Issole
Tarfaya
Wadi Bahloul
Gongzha

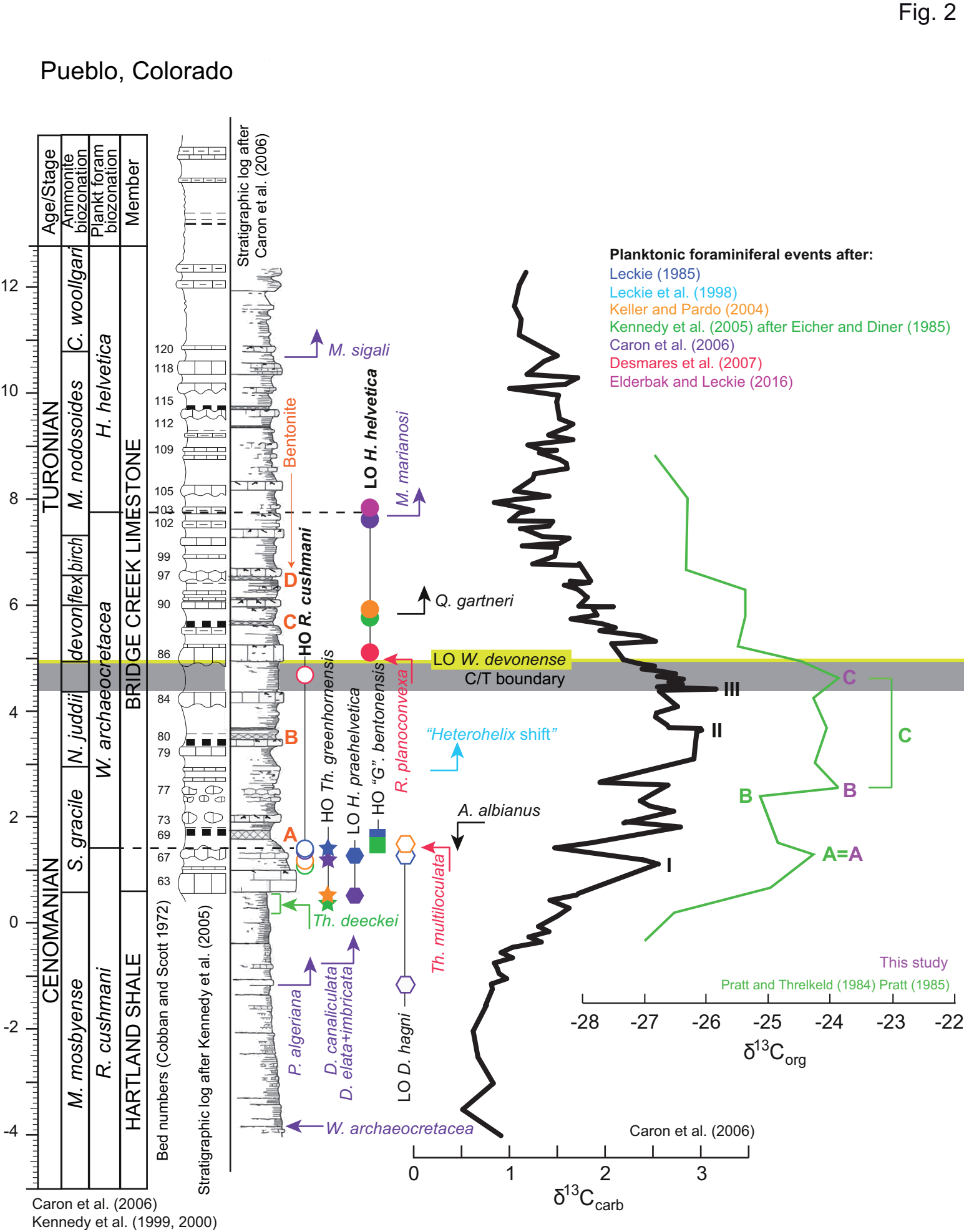
Pueblo, Colorado
Age/Stage
Ammonite biozonation
Plankt foram biozonation
Member
CENOMANIAN
TURONIAN
M. mosbyense
S. gracile
N. juddii
devon
flex
birch
C. woollgari
M. nodosoides
R. cushmani
W. archaeocretacea
H. helvetica
HARTLAND SHALE
BRIDGE CREEK LIMESTONE
Bed numbers (Cobban and Scott 1972)
Stratigraphic log after Kennedy et al. (2005)
Stratigraphic log after Caron et al. (2006)
Bentonite
M. sigali
LO H. helvetica
M. marianosi
Q. gartneri
HO R. cushmani
LO W. devonense
C/T boundary
HO Th. greenhornensis
LO H. praehelvetica
HO "G". bentonensis
R. planoconvexa
"Heterohelix shift"
A. albianus
Th. multiloculata
Th. deeckei
P. algeriana
D. canaliculata
D. elata+imbricata
LO D. hagni
W. archaeocretacea
A
B
C
D
I
II
III
Planktonic foraminiferal events after:
Leckie (1985)
Leckie et al. (1998)
Keller and Pardo (2004)
Kennedy et al. (2005) after Eicher and Diner (1985)
Caron et al. (2006)
Desmares et al. (2007)
Elderbak and Leckie (2016)
This study
Pratt and Threlkeld (1984) Pratt (1985)
δ13Corg
Caron et al. (2006)
δ13Ccarb
Caron et al. (2006)
Kennedy et al. (1999, 2000)

Fig. 3

Eastbourne (England)

Planktonic foraminiferal events after:

Paul et al. (1999)
Keller et al. (2001)
Hart et al. (2002)
Tsikos et al. (2004)
this study

$\delta^{13}C_{carb}$

3 4 5

Carbon-isotope profile and peaks after:

Paul et al. (1999)
Tsikos et al. (2004)
Jarvis et al. (2006)
Voigt et al. (2008)

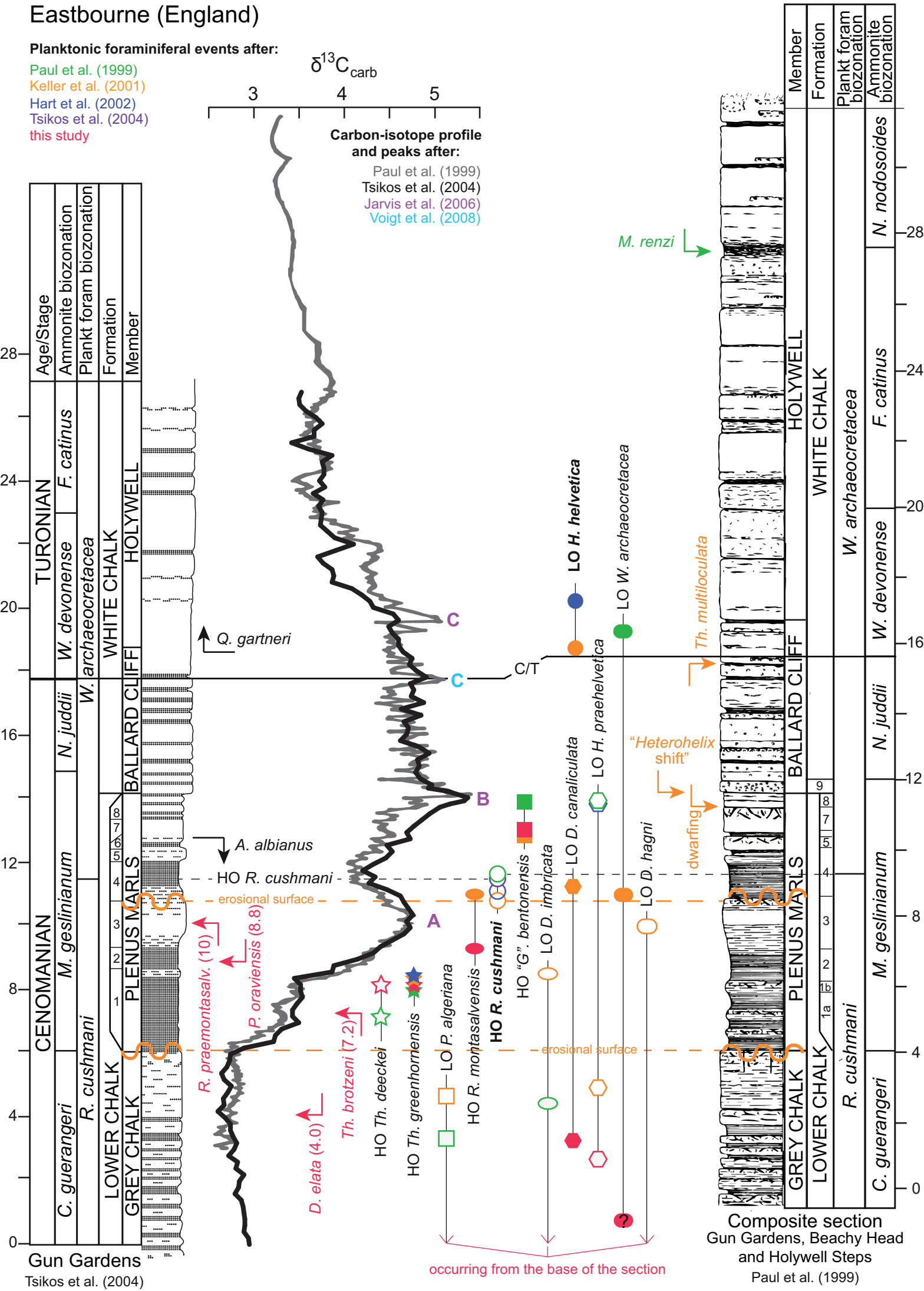

Gun Gardens
Tsikos et al. (2004)

Composite section
Gun Gardens, Beachy Head and Holywell Steps
Paul et al. (1999)

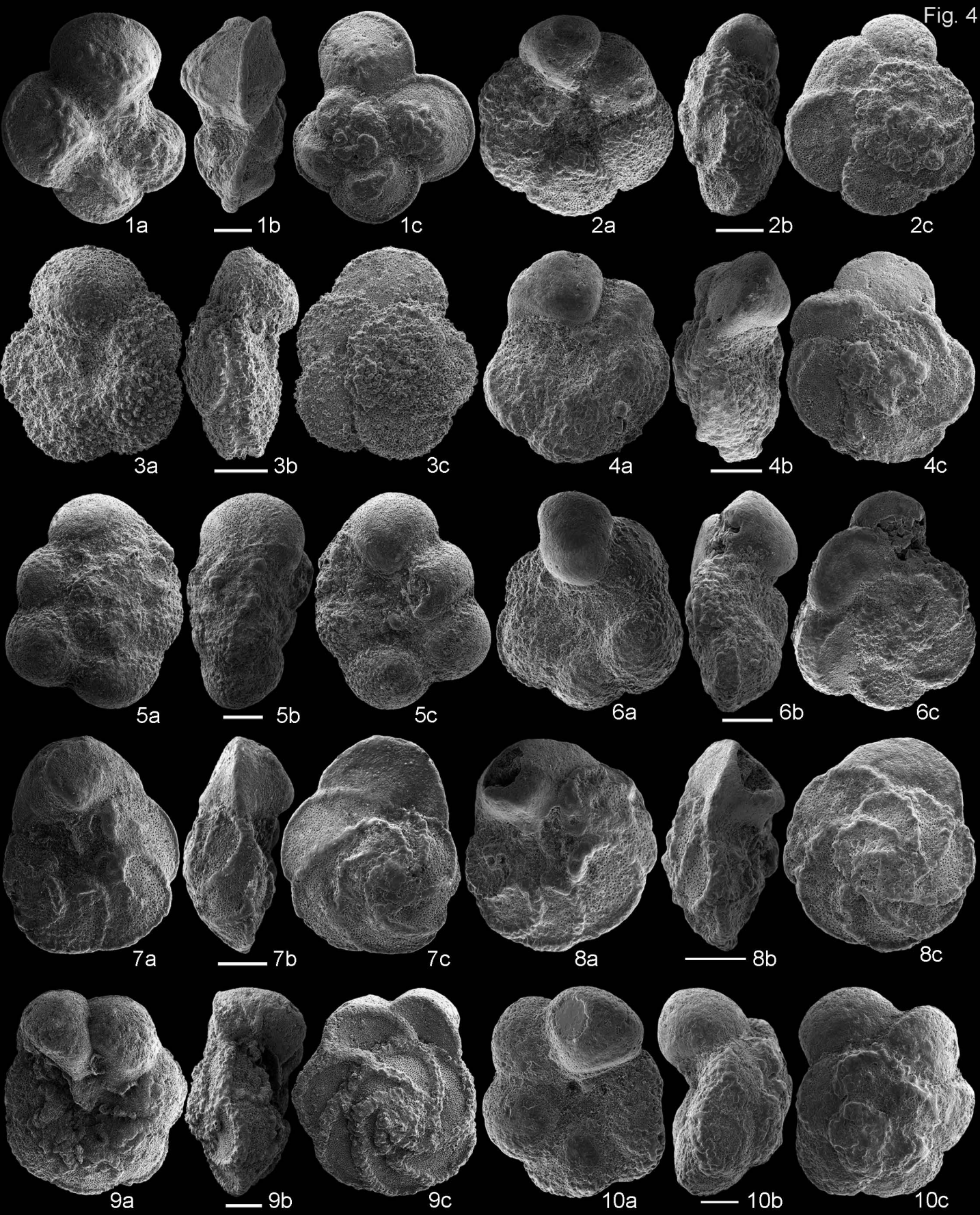
Fig. 4
1a
1b
1c
2a
2b
2c
3a
3b
3c
4a
4b
4c
5a
5b
5c
6a
6b
6c
7a
7b
7c
8a
8b
8c
9a
9b
9c
10a
10b
10c

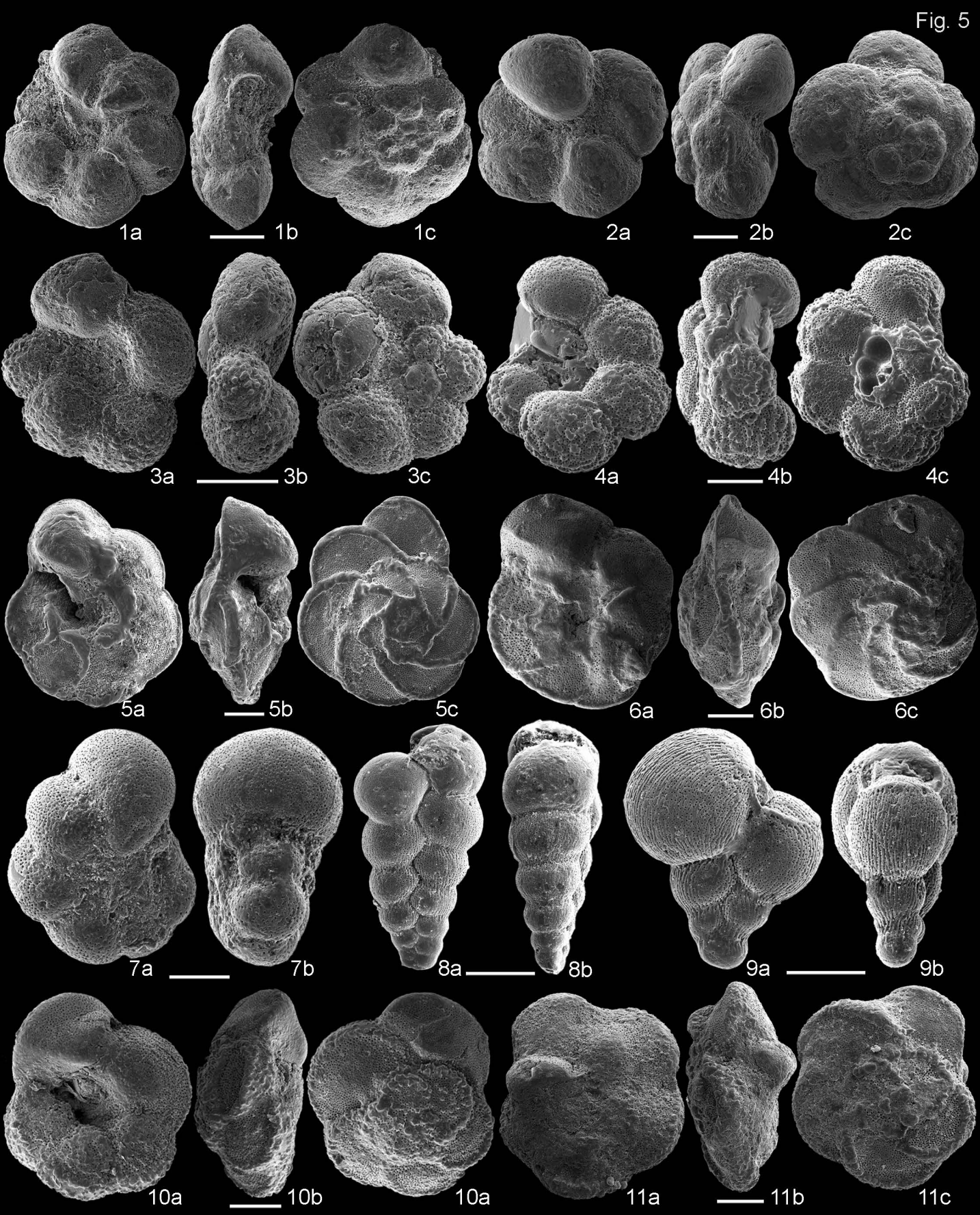
Fig. 5
1a
1b
1c
2a
2b
2c
3a
3b
3c
4a
4b
4c
5a
5b
5c
6a
6b
6c
7a
7b
8a
8b
9a
9b
10a
10b
10a
11a
11b
11c

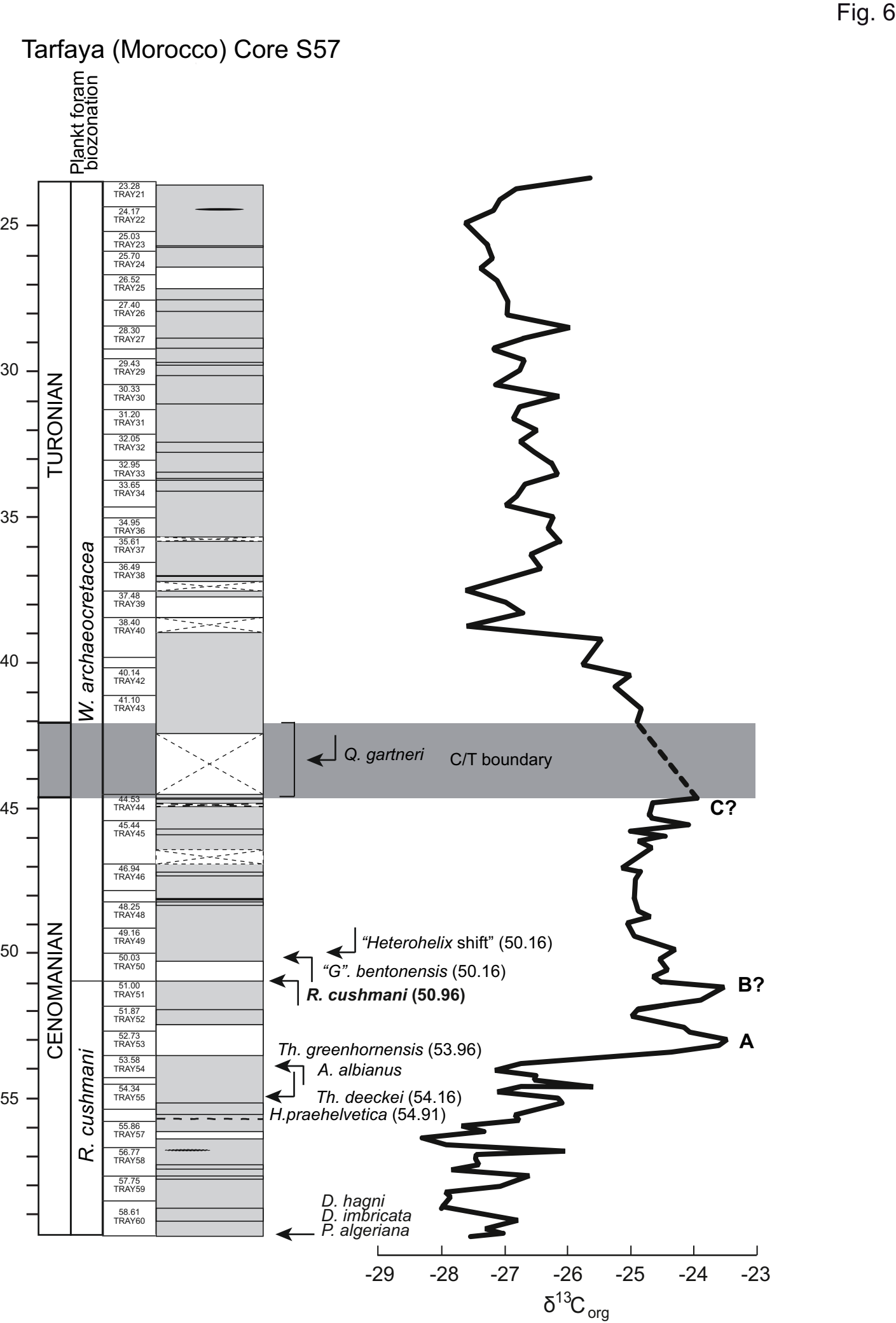
Tarfaya (Morocco) Core S57
Plankt foram biozonation
TURONIAN
CENOMANIAN
W. archaeocretacea
R. cushmani
23.28 TRAY21
24.17 TRAY22
25.03 TRAY23
25.70 TRAY24
26.52 TRAY25
27.40 TRAY26
28.30 TRAY27
29.43 TRAY29
30.33 TRAY30
31.20 TRAY31
32.05 TRAY32
32.95 TRAY33
33.65 TRAY34
34.95 TRAY36
35.61 TRAY37
36.49 TRAY38
37.48 TRAY39
38.40 TRAY40
40.14 TRAY42
41.10 TRAY43
44.53 TRAY44
45.44 TRAY45
46.94 TRAY46
48.25 TRAY48
49.16 TRAY49
50.03 TRAY50
51.00 TRAY51
51.87 TRAY52
52.73 TRAY53
53.58 TRAY54
54.34 TRAY55
55.86 TRAY57
56.77 TRAY58
57.75 TRAY59
58.61 TRAY60
25
30
35
40
45
50
55
Q. gartneri
C/T boundary
"Heterohelix shift" (50.16)
"G". bentonensis (50.16)
R. cushmani (50.96)
Th. greenhornensis (53.96)
A. albianus
Th. deeckei (54.16)
H.praehelvetica (54.91)
D. hagni
D. imbricata
P. algeriana
C?
B?
A
-29
-28
-27
-26
-25
-24
-23
δ13Corg

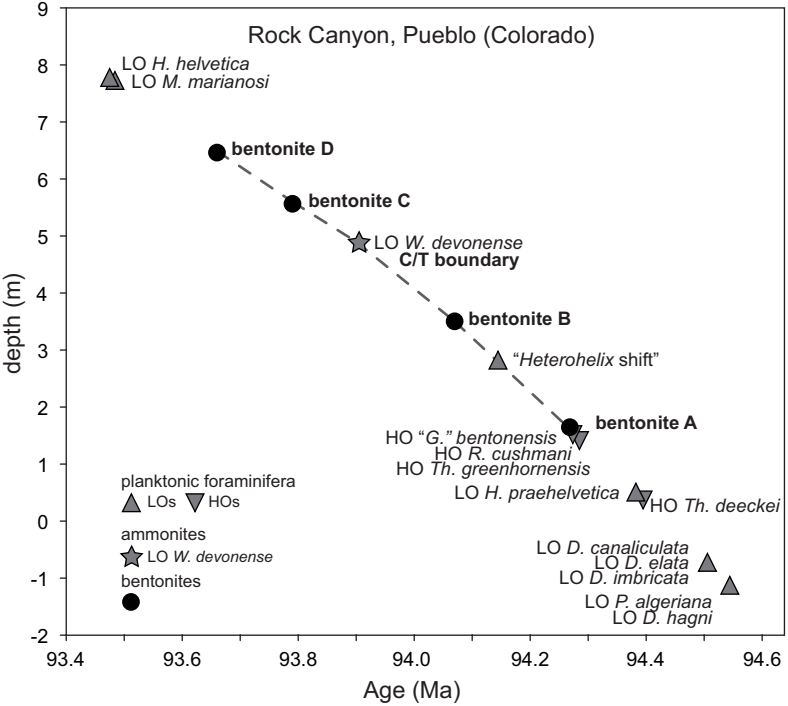
Rock Canyon, Pueblo (Colorado)
LO H. helvetica
LO M. marianosi
bentonite D
bentonite C
LO W. devonense
C/T boundary
bentonite B
"Heterohelix shift"
bentonite A
HO "G." bentonensis
HO R. cushmani
HO Th. greenhornensis
LO H. praehelvetica
HO Th. deeckei
LO D. canaliculata
LO D. elata
LO D. imbricata
LO P. algeriana
LO D. hagni
planktonic foraminifera
LOs
HOs
ammonites
LO W. devonense
bentonites
depth (m)
Age (Ma)
9
8
7
6
5
4
3
2
1
0
-1
-2
93.4
93.6
93.8
94.0
94.2
94.4
94.6

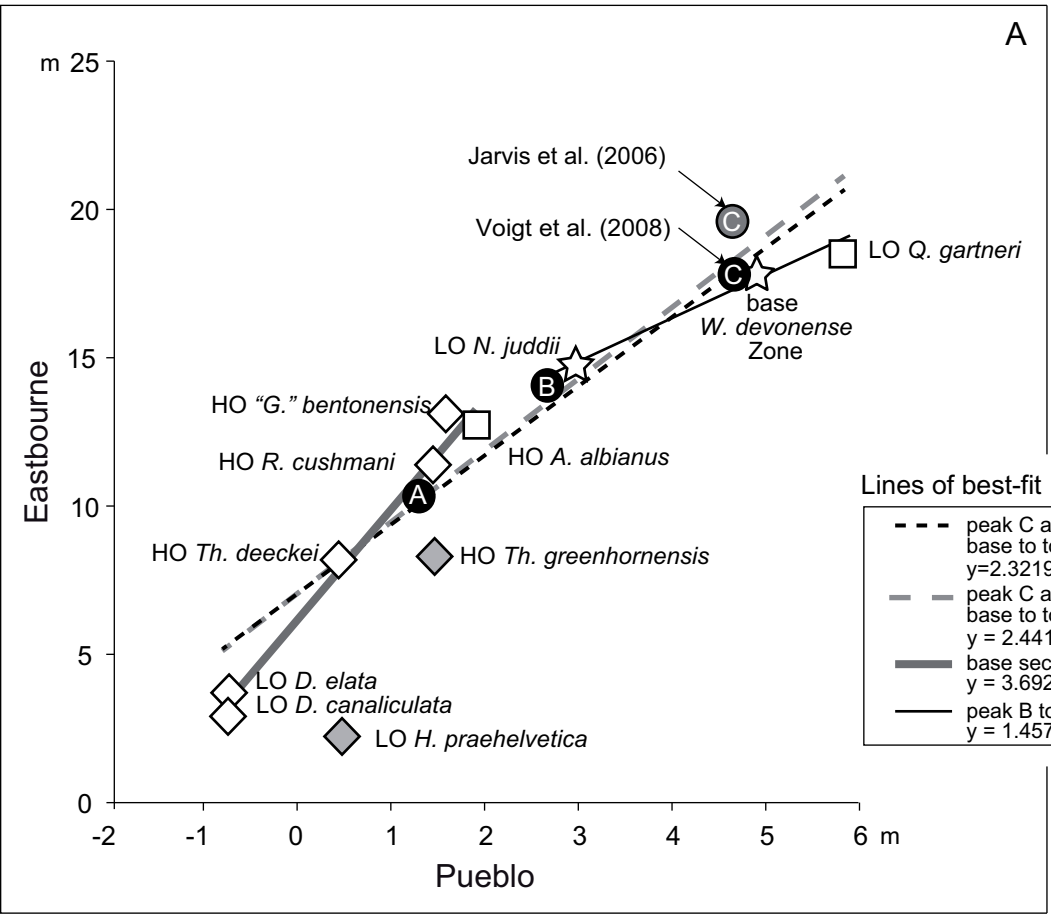

Symbols

- Chemostratigraphic events
- Planktonic foraminiferal events used to calculate the regression line
- Planktonic foraminiferal events *not* used to calculate the regression line
- Calcareous nannofossil events
- Ammonite events

Lines of best-fit

- peak C at Eastbourne according to Voigt et al. (2008) base to top section
  y=2.3219x+7.148; R^2=0.92105
- peak C at Eastbourne according to Jarvis et al. (2006) base to top section
  y = 2.4419x + 6.8633; R^2 = 0.90849
- base section to HO "*G." bentonensis* and HO *A. albianus*
  y = 3.6921x + 6.2984; R^2 = 0.97513
- peak B to top section (C according to Voigt et al. 2008)
  y = 1.4576x + 10.563; R^2 =0.96072

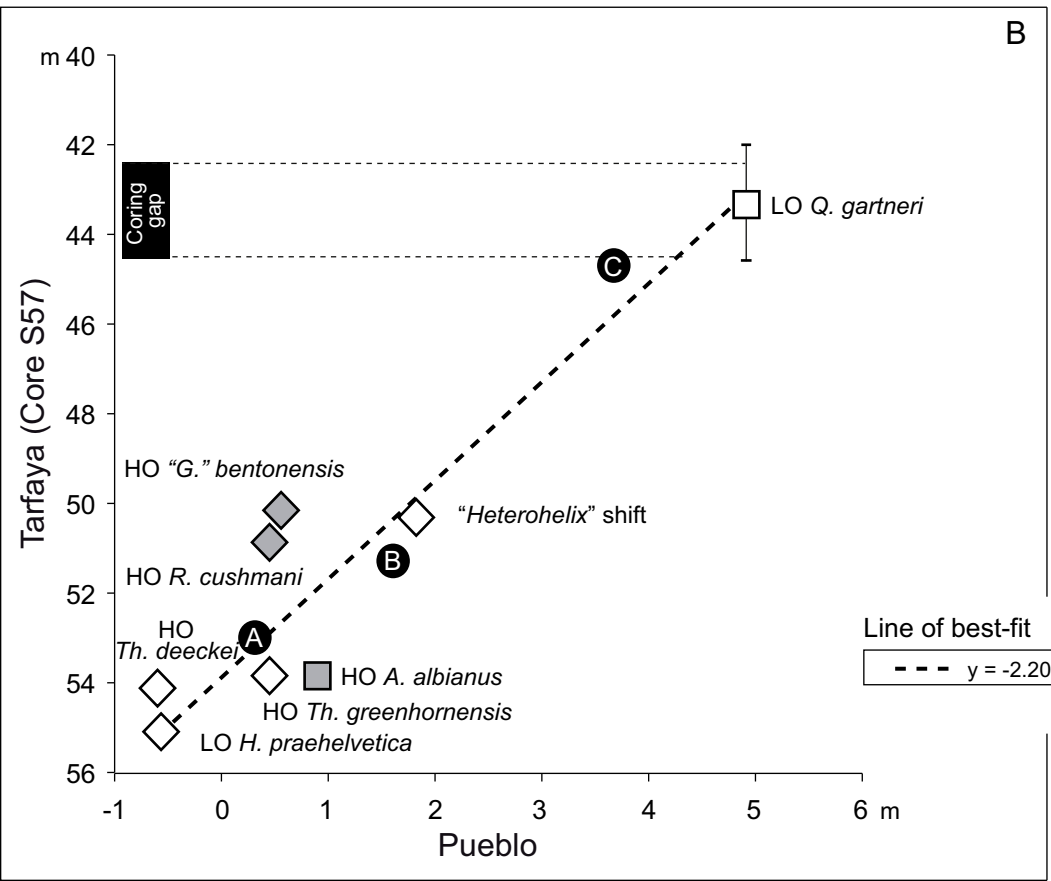

Symbols

- Chemostratigraphic events
- Planktonic foraminiferal events used to calculate the regression line
- Planktonic foraminiferal events *not* used to calculate the regression line
- Calcareous nannofossil events used to calculate the regression line
- Calcareous nannofossil events *not* used to calculate the regression line

y = -2.2091x + 56.028
R^2 = 0.96711

Line of best-fit

- y = -2.2091x + 56.028; R^2 =0.96711

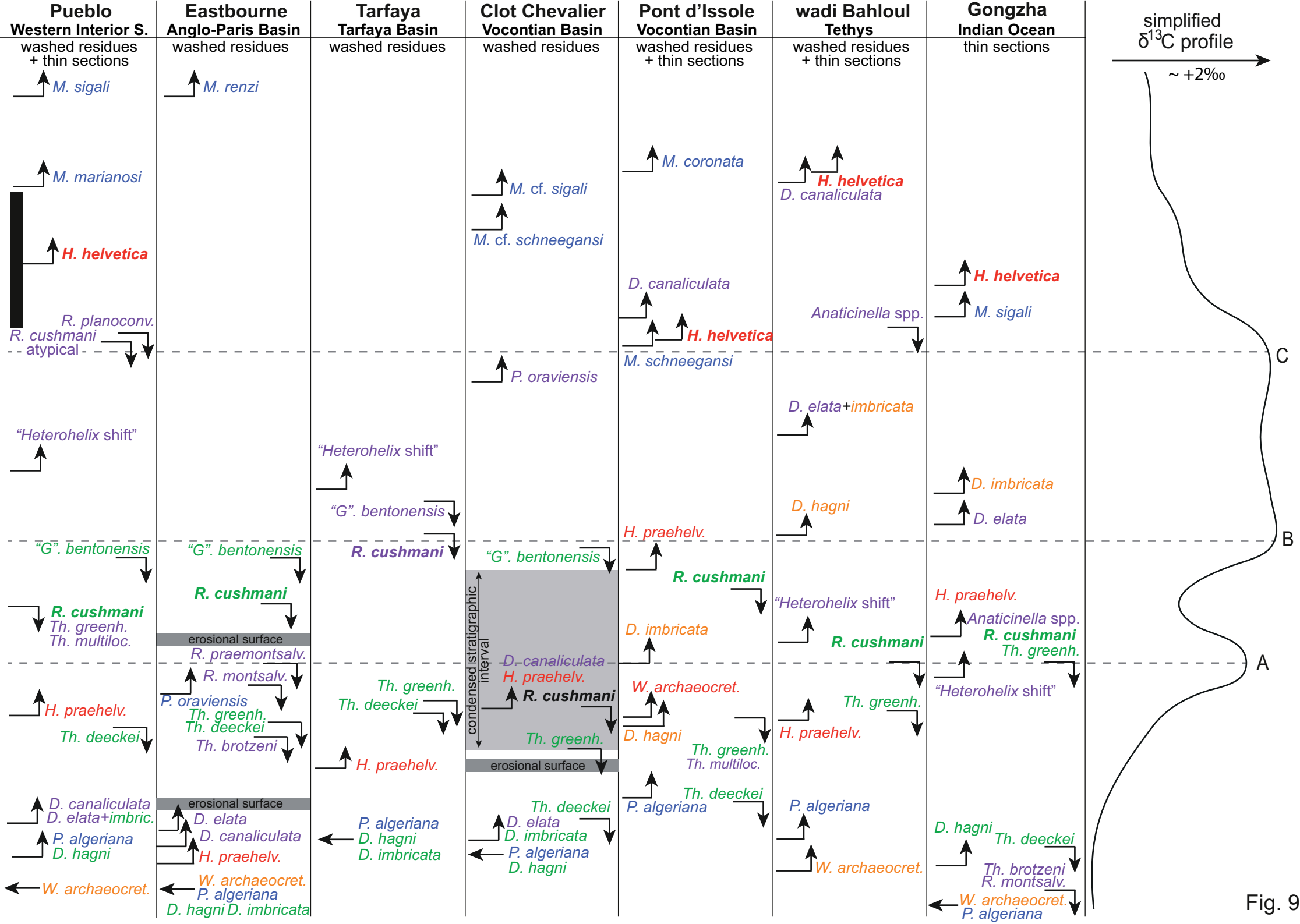
Pueblo
Western Interior S.
washed residues + thin sections
M. sigali
M. marianosi
H. helvetica
R. planoconv.
R. cushmani
atypical
"Heterohelix shift"
"G". bentonensis
R. cushmani
Th. greenh.
Th. multiloc.
H. praehelv.
Th. deeckei
D. canaliculata
D. elata+imbric.
P. algeriana
D. hagni
W. archaeocret.
Eastbourne
Anglo-Paris Basin
washed residues
M. renzi
"G". bentonensis
R. cushmani
erosional surface
R. praemontsalv.
R. montsalv.
P. oraviensis
Th. greenh.
Th. deeckei
Th. brotzeni
erosional surface
D. elata
D. canaliculata
H. praehelv.
W. archaeocret.
P. algeriana
D. hagni
D. imbricata
Tarfaya
Tarfaya Basin
washed residues
"Heterohelix shift"
"G". bentonensis
R. cushmani
Th. greenh.
Th. deeckei
H. praehelv.
P. algeriana
D. hagni
D. imbricata
Clot Chevalier
Vocontian Basin
washed residues
M. cf. sigali
M. cf. schneegansi
P. oraviensis
"G". bentonensis
condensed stratigraphic interval
D. canaliculata
H. praehelv.
R. cushmani
Th. greenh.
erosional surface
Th. deeckei
D. elata
D. imbricata
P. algeriana
D. hagni
Pont d'Issole
Vocontian Basin
washed residues + thin sections
M. coronata
D. canaliculata
H. helvetica
M. schneegansi
H. praehelv.
R. cushmani
D. imbricata
W. archaeocret.
D. hagni
Th. greenh.
Th. multiloc.
Th. deeckei
P. algeriana
wadi Bahloul
Tethys
washed residues + thin sections
H. helvetica
D. canaliculata
Anaticinella spp.
D. elata+imbricata
D. hagni
"Heterohelix shift"
R. cushmani
Th. greenh.
H. praehelv.
P. algeriana
W. archaeocret.
Gongzha
Indian Ocean
thin sections
H. helvetica
M. sigali
D. imbricata
D. elata
H. praehelv.
Anaticinella spp.
R. cushmani
Th. greenh.
"Heterohelix shift"
D. hagni
Th. deeckei
Th. brotzeni
R. montsalv.
W. archaeocret.
P. algeriana
simplified δ13C profile
~ +2‰
C
B
A

Fig. 9

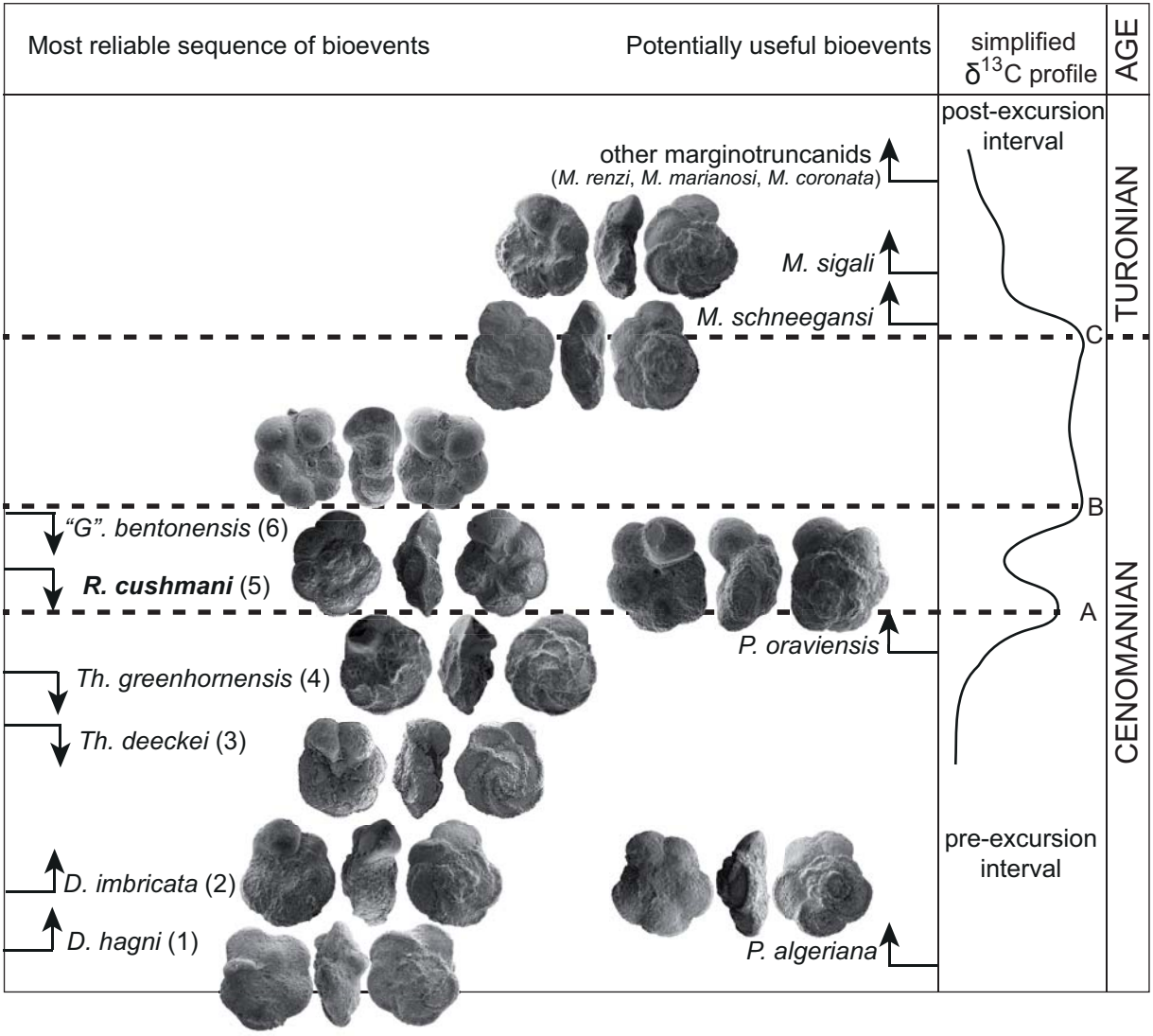
Most reliable sequence of bioevents
Potentially useful bioevents
simplified δ13C profile
AGE
post-excursion interval
other marginotruncanids
(M. renzi, M. marianosi, M. coronata)
M. sigali
M. schneegansi
TURONIAN
C
B
A
CENOMANIAN
"G". bentonensis (6)
R. cushmani (5)
P. oraviensis
Th. greenhornensis (4)
Th. deeckei (3)
pre-excursion interval
D. imbricata (2)
D. hagni (1)
P. algeriana

Fig. 11